X-633-63-50

53p.

THERMODYNAMICS OF SPACE FLIGHT

(HEAT TRANSFER PHENOMENA IN SPACE)

MARCH 25, 1963

GODDARD SPACE FLIGHT CENTER
GREENBELT, MD.

THERMODYNAMICS OF SPACE FLIGHT
(HEAT TRANSFER PHENOMENA IN SPACE)

by

Milton Schach and Robert E. Kidwell, Jr.

NASA Goddard Space Flight Center,

Greenbelt, Maryland

A lecture prepared for the
Space Environment Technology Series
conducted by
The Pennsylvania State University
~~in cooperation with the~~ and
Institute of Environmental Studies
Mid-Atlantic Chapter

25 March 1963

NOTICE

THIS DOCUMENT HAS BEEN REPRODUCED FROM THE BEST COPY FURNISHED US BY THE SPONSORING AGENCY. ALTHOUGH IT IS RECOGNIZED THAT CERTAIN PORTIONS ARE ILLEGIBLE, IT IS BEING RELEASED IN THE INTEREST OF MAKING AVAILABLE AS MUCH INFORMATION AS POSSIBLE.

Introduction

In this lecture we shall be concerned with heat transfer processes in that portion of the earth's atmosphere where the dominant mode of energy exchange between the environment and its contents is radiation. We shall emphasize primarily the thermal interaction between that environment and spacecraft placed in it. This region of interest begins at an altitude above the surface of the earth of approximately 100 miles, a height at which the lifetime of spacecraft can exceed at least one complete orbit. In the region above one hundred miles, aerodynamic heating effects are negligible. The density of all atomic or molecular particles is so low that they do not contribute measurably to the energy balance of any macroscopic body even though the particle velocities correspond to temperatures above 1000°K. Aerodynamic heating effects will be discussed in the next lecture.

This lecture will be divided into two parts. The first part will describe: (a) the characteristics of the external and internal radiant energy which contribute to the spacecraft energy balance and (b) the materials properties which govern the absorption and emission of energy by the spacecraft. The second part of the lecture, to be presented by Mr. Kidwell, will describe the spacecraft thermal design process and will include a discussion of the boundary conditions, formulation of the energy balance equations, computer solutions and the design of several Goddard spacecraft.

The external thermal environment of orbiting spacecraft consists of radiant energy from the sun, solar radiation reflected by the earth (or by any other celestial body near the spacecraft) and radiation emitted directly by the earth.

Solar Radiation

Two properties of the solar radiation are significant for us: (1) magnitude, (2) spectral distribution. The magnitude of the solar radiation incident on a one square centimeter surface placed normally to the radiation is 0.140

watts (corresponding to 130 watts ft^{-2}) at the mean distance of the earth from the sun[1]. This quantity is called the solar constant. Because the earth's orbit is elliptical, the earth-sun distance varies and this incident power can range from 96.5 to 103.5% of the mean value. The incident power varies inversely as the square of the distance so that the corresponding mean values for the planets Mars, Venus and Mercury are 0.435, 1.94 and 6.7 times the earth's solar constant, respectively. The solar constant is known to an accuracy of about ±2%. Measurements of the solar constant have been made both on the ground and at various altitudes, for over a period of 60 years. These measurements indicate that the solar constant is, indeed, invariant, even though large changes can occur over very narrow bands of the solar spectrum during periods of solar activity. The past 15 years of high altitude rocket measurements have extended our knowledge of the solar spectrum into the ultraviolet region. Most of the radiation below 0.3 micron wave length is absorbed in the earth's atmosphere and could not be detected at sea level. The net effect of these high altitude measurements has been to increase our estimate of the solar constant from 0.136 to 0.140 watts cm^{-2}. The distribution of the solar energy into its spectral components is shown in Figure 1. The solar energy is spread over a vast spectral range from the ultra-x-ray to the far infra-red. However, the spectral range, significant as a thermal environment, may be considered to extend from 0.3 to 4.0 microns. This arbitrarily selected region excludes about 1% of the total solar energy above and 1% below its limits. If the upper limit is reduced to 2.6 microns, an additional 2% of the total solar energy is excluded.

There is no simple equation which accurately describes the solar spectral intensity as a function of wave length. The spectral intensity curve of a black body radiating between 5700° and 6000°K does show a fair resemblance to the solar curve. The shape of the solar curve in the visible and near infrared regions, say from about 0.4 to 1.2 microns, is best matched by the black body curve at 6000°K. The curve for the radiating black body at 5760°K shows a poorer match in this spectral region but the total energy radiated by a unit area at this temperature equals the solar constant. (We shall return to the concept of black body radiation on page 4.)

Thermal Equilibrium and Solar Radiation

Before examining the other sources of radiation which complete the environment, let us consider the thermal effect of solar radiation alone on a body in space and describe the condition of equilibrium. In general, some of the incident solar radiation will be absorbed, some transmitted through the body and the remainder reflected from the surface. In addition, the body emits radiation. The body will exist in thermal equilibrium when the rate at which solar energy is absorbed equals the rate at which the body emits radiation. We shall need two definitions: (1) solar absorptance and (2) thermal emittance, in order to determine the effect of solar radiation on the thermal balance.

Solar Absorptance

The fraction of incident solar radiation absorbed by the body is called its solar absorptance and is designated by the letter "a". Values of "a" range from a low of 0.045 for freshly evaporated silver on an optically smooth surface to 0.95 for some black paints. Values approaching 0.98 have been achieved by carefully prepared thin multiple films of evaporated aluminum and silicon monoxide. The absorptance of a material depends not only on an intrinsic quality associated with the underlying molecular structure, but also on the smoothness of the surface of the material. Thus, metals like silver, aluminum, and gold evaporated in films a few tenths of a micron thickness on optically smooth surfaces are opaque to solar radiation and reflect about 95, 92, and 81 per cent of the solar radiation (0.3 to 3 micron range) respectively; their corresponding absorptances are 5, 8 and 19%, respectively. Indentations in their surface will increase the radiation absorbed. The increased absorption comes about as a result of the fact that some of the reflected radiation is intercepted by other portions of the surface and multiple absorption occurs. Figure 2 illustrates this idea. In a recent experiment flown on an orbiting solar observatory, a highly absorbing surface was constructed with thin razor blades. The wedge-shaped cavities formed by the ends of the blades effectively trapped more than 90 per cent of the normally incident solar radiation. Surfaces painted with a brush will commonly exhibit higher absorptances than the same surfaces sprayed with the identical paint because of the indentations produced by the brush.

Thermal Emittance

The ability of a body to emit radiation depends on its temperature and on a parameter called its thermal emittance. We designate the latter by the letter "e". Values of "e" range from approximately 0.02 for evaporated silver to 0.95 for some non-metallic paints. Thermal emittance, like solar absorptance, depends on smoothness, but as we shall see shortly, longer wave length radiation is involved, and larger surface irregularities are required to trap thermal radiation. The total radiation emitted, P, by a surface of unit area can be represented by the equation

$$P = e\sigma T^4 \qquad (1)$$

where the undefined quantities are:

σ = Stefan-Boltzmann constant

T = absolute temperature of the surface

We designate as a black body, a surface for which e = 1.0. All other surfaces at the same temperature will emit less radiation. Black body radiation can be approached very closely by the radiation leaving a small opening of a body maintained at a uniform temperature. The concept of a black body radiator will be useful to us as a reference. The power radiated by a black body for a few temperatures is shown below:

T^o Kelvin	P watts cm^{-2}	P watts ft^{-2}
250^o	23.9×10^{-3}	21.2
300^o	47.5×10^{-3}	44.0
350^o	88.0×10^{-3}	82.0
400^o	150.0×10^{-3}	139.0

The concept of a black body is also useful to us because of its defined spectral intensity distribution, given by Planck's law:

$$I_\lambda = \frac{c_1 \lambda^{-5}}{e^{c_2/\lambda T} - 1} \qquad (2)$$

where the new symbols are:

I_λ = radiated power per unit area and per unit wave length interval at wave length λ

λ = wave length

c_1 and c_2 are constants

A plot of spectral intensity distribution for black body radiating surfaces is shown in Figure 3. The curve for 288°K, corresponding to room temperature, shows that the bulk of the radiant energy is emitted between 5 and 50 microns; one per cent lies below 5 microns, 12 per cent lies above 30 microns, 3 per cent lies above 50 microns, and the peak intensity occurs at 10 microns. At 100°C., one per cent of the radiated energy is excluded below 3.8 microns, three per cent above40 microns, and the peak intensity occurs at 7.7 microns. Actual surfaces will emit less radiation at any given wave length and temperature than a black body, but this radiation is confined to the same spectral region. We can now redefine the thermal emittance as the ratio of radiation emitted by the surface to that emitted by a black body at the same temperature.

Examples of Thermal Equilibrium with Solar Radiation

Our discussion up to this point has described solar radiation, the dominant external source, and the radiation emitted by a body near room temperature. We have seen that the solar radiation lies in one spectral region, 0.3 to 3 microns, and the radiation of a body at or near room temperature radiates in a region from 3 to 50 microns approximately. We can anticipate that when we consider the two other components of the radiation environment: (1) solar radiation reflected by the earth and (2) the earth's emitted radiation, that the same two spectral regions will be important.

Consider next several simple illustrations of bodies in equilibrium. The solar radiation absorbed must equal the longer wave radiation emitted, thus

$$A_s sa = A \sigma e T^4 \qquad (3)$$

where the undefined symbols are:

A_s = the area perpendicular to the solar radiation

s = solar constant

A = total area emitting radiation

Solving for T gives:

$$T = \left[\frac{A_s}{A} \quad \frac{s}{\sigma} \quad \frac{a}{e} \right] \qquad (4)$$

Equation (4) can be applied to a number of special cases to yield an average temperature. As an example, consider a sphere. A spherical body in equilibrium with solar radiation will, in general, exhibit a temperature gradient because of the difference in absorbed energy for the various surface elements which, in turn, follows from the variation in angle between the incident radiation and these surface elements. Nevertheless, the energy balance permits this equation to be solved for an average temperature, the root mean fourth temperature over the surface. This temperature would be observed experimentally in the interior of a hollow sphere. Equation (4) indicates the importance of the geometric factor, A_s/A, and the ratio of radiation properties, a/e, for equilibrium temperatures.

Case 1.

A sphere coated with evaporated aluminum.
$a = 0.10, \quad e = 0.025$

$$\frac{A_s}{A} = \frac{\pi r^2}{4\pi r^2} = \frac{1}{4} \quad \frac{s}{\sigma} = 243 \times 10^8 \quad \frac{a}{e} \quad \frac{1}{4}$$

$$T^4 = 243 \times 10^8$$

$$T = 395^\circ K = 122^\circ C$$

Case 2.

A sphere painted black. a = 0.9, e = 0.9

$$T = 279^\circ K = 6^\circ C$$

Case 3.

A sphere with a = 0.65, e = 1.0,

$$T = 250^\circ K = -23^\circ C$$

Case 4.

A sphere painted white. a = 0.30, e = 0.90

$$T = 212^\circ K = -61^\circ C$$

Case 5.

A flat plate perpendicular to the sun's rays; evaporated aluminum on both faces. a = 0.10, e = 0.025

$$T = 469^\circ K = 196^\circ C$$

Case 6.

Same as Case 5, except face away from sun is painted black. a = 0.10, e_f = 0.025, e_b = 0.90

$$T = 227^\circ K = -46^\circ C$$

Case 7.

A flat plate, perpendicular to the sun's rays; black paint on both faces. a = 0.9, e = 0.9

$$T = 332^{\circ}K = 59^{\circ}C$$

Case 8.

A flat plate, perpendicular to the sun's rays; black paint on sun viewing face, evaporated aluminum on back face.

$$T = 392^{\circ}K = 119^{\circ}C$$

Solar Radiation Reflected by the Earth

The second component of the external radiation environment to be considered is the solar radiation which the earth reflects. The fraction of incident solar power which the earth returns to space is called its "albedo". Solar radiation is returned to space by scattering in the atmosphere and by reflection from clouds and from the surface. The processes are extrememly complex in detail. Scattering by the atmosphere occurs at all altitudes. The cloud cover varies in time and space. Cloud reflectances vary from 20 to 70 per cent. The surface of the earth is characterized by a wide range of reflectances as shown in the following table[2].

	Fraction of incident sunshine reflected
Forests	.07
Bushes	.10
Fresh Snow	.70
Water	.07 (for incident angles less than 65°)
Grass	.10 to .15

Detailed studies of the meteorological data by H. Houghton, S. Fritz and others give a value of 34 or 35 per cent for the average earth albedo. An independent measurement of the average albedo has been undertaken by the French astronomer, Danjon. His comparison of the brightness of the portions of the moon which are illuminated (1) by the sun directly, and (2) by earth reflected solar radiation, gives an albedo value of 35 per cent. The albedo radiation, on the average, is composed of 25% cloud reflection, 7% atmospheric scattering and 2% surface reflected radiation. (The percentages refer to the total incident solar radiation). Houghton[3] has computed albedo values as a

function of latitude for the northern hemisphere as follows:

Latitude	0	10	20	30	40	50	60	70	80	90
Albedo	.326	.310	.283	.284	.335	.389	.443	.527	.602	.669

Precise knowledge of the spectral intensity distribution of the albedo radiation is lacking. Calculations of the albedo spectrum based on the work of S. Fritz, and knowledge of the spectral reflectance of clouds and atmospheric scattering, have been undertaken recently. Experiments for the measurement of this spectrum are planned in the near future. In the absence of more accurate information, the albedo spectrum is assumed to be identical with the solar spectrum. The magnitude of the albedo radiation will be discussed under the orbital factors.

Earth Emitted Radiation

The last component of the external environment to be considered is the earth emitted radiation. In the last section we noted that the earth reflects about 35% of the incident solar radiation. If, as we believe, the earth is in thermal equilibrium, 65% of the incident solar radiation is absorbed, and an equal amount of power must be emitted. The temperature over the surface of the earth ranges from approximately -40 to +40°C; the mean surface temperature is about +14°C. The radiation emitted by the surface lies predominantly in the region above 5 microns. The atmospheric water vapor and carbon dioxide absorb all the surface emitted radiation except for a band from 7 to 14 microns. The atmosphere partially absorbs the radiant energy between 7 and 8.5 and between 11 and 14 microns. The radiation between 8.5 and 11 microns is transmitted to space with little attenuation. The layers of the atmosphere will emit and absorb radiation until an altitude is reached where the water vapor and carbon dioxide depletion occurs, and black body radiation corresponding to the temperatures of these upper layers (-55 to -60°C) is emitted to space. The solid curve in Figure 3 shows the estimated composite spectral intensity distribution. The magnitude of the earth emitted radiation will be discussed in the next section.

Orbital Factors, Albedo and Earth-Emitted Radiation

We have, thus far, described the thermal radiation sources. The impact of this environment will depend on the orbit or trajectory and on the configuration and thermal properties of the spacecraft.

It was pointed out earlier that the magnitude of the incident solar radiation varies ±3% with the earth distance from the sun. By far the most significant orbital parameter is the fraction of the orbital period which is spent in sunlight. For near earth orbits, this fraction can vary from about .60 to 1.00; during the remainder of the orbital period, the spacecraft is in the earth's shadow. The percent of period in sunlight for elliptical orbits depends on the eccentricity, semi-major axis, location of perigee, and angle between the normal to the orbital plane and the sun-earth line. The percent of time in sunlight increases as the angle between orbital plane and earth-sun line decreases. The initial percent time in sunlight is illustrated in Figure 4 as a function of the launching time.[4] By selecting the launch time, the initial position of perigee and the initial angle between the orbital plane normal and earth-sun line is virtually fixed. In general, the orbit will precess because of the earth's equatorial bulge and the perigeal point will advance along the orbit. These orbital changes will produce changes in the percent of time spent in sunlight. Figure 5 shows how the average temperature of a spherical satellite is affected primarily by the percent of the orbital period in sunlight.[5]

We wish to discuss next the magnitude of the albedo radiation which may be incident on a spacecraft. It will be recalled that the albedo energy varies with the reflectance of the particular surface. A range of 7 to 70 percent of the incident solar energy has been noted for clouds and ground elements. In principle, if the albedo of the earth is known as a function of latitude and longitude, the incident albedo energy on a surface element in orbit can be computed. In practice, the uncertainty in cloud cover makes a precise calculation virtually impossible. What can be done is to compute for an average value of reflectance. The albedo radiation on a satellite will then depend on its height above the earth and position with respect to the sunlit half of the earth. This position is defined by the angle between the sun-earth line and the satellite-earth line; it is

understood that these lines are drawn between centers of the respective bodies, i.e., the earth-sun line is drawn between sun-center and earth-center. The results of calculation by F. Cunningham of the earth-reflected solar power incident on a sphere of unit cross-section area is shown in Figure 6[5]. θ_s in the figure is the angle just defined. θ_s equal to zero is the sub-polar point on the earth's surface, i.e., the point on the earth's surface produced by intersection of the earth-sun line with the earth's surface. For an assumed albedo of 0.34, we see that the incident earth-reflected sunshine equals about one-half the direct solar radiation at a 125-mile altitude. The albedo radiation decreases to less than 2 percent of the direct solar radiation as we approach 32,000 kilometers (20,000 miles) altitude or as we increase θ_s to 90°.

The earth-emitted radiation, to which we now turn, presents some of the same difficulties as does the albedo. We have seen that the earth reflects about 35% of the incident solar radiation and absorbes 65% which the earth emits as long wave radiation. In Case 3 (page 7), we calculated the mean temperature of a sphere which absorbed 65% of the incident solar radiation and emitted with e = 1.0. For the earth, "e" must lie between 0.9 and 1.0 (70% of the earth's surface is water having an "e" value equal to 0.95). Our calculation gave T = 250°K (-23°C). This value may be a good one for the average planetary temperature if we recall that the average surface temperature is +14°C and the temperature of the upper atmosphere, which radiates to space, is about -60°C. From our table (page 4) of the radiation emitted by a black body, we see that the earth emits, on the average, almost 24 x 10^{-3} watts cm^{-2} (21.2 watts ft^{-2}). The earth-emitted radiation incident on a sphere of unit cross-section area as a function of altitude is shown in Figure 7. The earth-emitted radiation incident on a flat plate is shown in Figure 8, where the angle between the normal to the plate and the plate-earth center line is a parameter. The earth-emitted radiation incident on a sphere at 20,000 miles is less than 2% of the direct solar radiation.

Factors Affecting Radiation Properties Required for Coating

In the preceding discussion we have seen that two radiometric properties of spacecraft surfaces, the solar absorptance and thermal emittance, play a major role in establishing the thermal balance in orbit. The range of properties available and a few examples of coating materials were mentioned. In the remaining portion of this half of the lecture, I propose to consider, qualitatively or semi-quantitatively, the factors influencing the values of solar absorptance and thermal emittance which are selected. We will be concerned with both the a/e ratios as well as their absolute values.

(1) We consider first the effects of the temperature limits which may be tolerated. In general, high temperatures will tend to require high ratios of a/e and low temperatures will contribute to low a/e values. Our previous examples of spheres in equilibrium with solar radiation showed that temperatures of -61°, 6° and 122°C correspond to a/e values of 0.3, 1.0 and 4.0, respectively. This factor suggests no preference for low or high absolute values of a and e.

(2) We consider next the effect of the magnitude of the internal dissipation. As the value of internal dissipation increases, higher emittance values are needed. The effect of the internal power dissipation on the average temperature can be obtained for simple configurations in equilibrium as follows:

If P_i is the internal dissipation, then equation (3) becomes

$$A_s\, sa + P_i = A\sigma eT^4 \qquad (5)$$

Introducing the definitions

$$P_i = p_i A \qquad \text{and} \qquad k = p_i/s$$

where P_i is the internal power dissipation per unit surface area and k describes the internal power dissipation density in terms of the solar radiation density, equation (5) can be written

$$A_s\, sa + Aks = A\sigma eT^4 \qquad (6)$$

and

$$T^4 = \left(\frac{A_s a}{A} + k\right) \frac{s}{\sigma e} \tag{7}$$

and for the case of the sphere $A_s/A = 1/4$, and

$$T^4 = \left(\frac{a}{4} + k\right) \frac{s}{\sigma e} \tag{8}$$

The relation between e for any internal dissipation and temperature T to e_o, the case for zero internal dissipation and the same temperature T is obtained by equating T^4 from equation (3) to T^4, equation (8).

$$T^4 = \left(\frac{a}{4} + k\right) \frac{s}{\sigma e} = \frac{a}{4} \frac{s}{\sigma e_o} \tag{9}$$

$$e/e_o = 1 + \frac{4k}{a} \tag{10}$$

It also follows for a sphere of given a and e that the relation between the T^4 and T_o^4, corresponding to the cases with and without internal dissipation, is

$$T^4/T_o^4 = 1 + 4k/a \tag{11}$$

The effects of internal dissipation on temperature and on thermal emittance for the case of a sphere are shown for a few values of a and k in the table on page 14.

	1	2	3	4	5	6	7	8
a	1	1	1	0.15	0.15	0.15	0.15	0.15
e	1	1	1	0.15	0.15	0.25	0.15	1.0
k	0	1/40	1/4	0	1/40	1/40	1/4	1/4
T^4	60.7×10^8	67×10^8	121×10^8	60.7×10^8	101×10^8	60.7×10^8	467×10^8	69.9×10^8
$T^{\circ}K$	279	285	332	279	317	279	465	289
$T^{\circ}C$	$6^{\circ}C$	$12^{\circ}C$	$59^{\circ}C$	$6^{\circ}C$	$44^{\circ}C$	$6^{\circ}C$	$192^{\circ}C$	$13^{\circ}C$

The third factor to be considered is the temperature gradient over the spacecraft. In general, the incident and absorbed energies on each element of the spacecraft will vary with position on the surface. The gradient is affected by many factors: spin or zero spin, orientation of spin axis with respect to the sun, possibility of radiant heat transfer within the spacecraft, thermal conduction between high and low energy absorbing surface elements, and internal dissipation distribution. To gain a little insight into the problem, we shall examine the temperature distribution of a simple configuration.

Consider a spherical shell without spin (or spinning with its axis parallel to the sun's rays) in equilibrium with solar radiation. Three restrictions will be made: (1) no gradient in the radial direction exists; (2) the inner surface of the shell emits (and reflects) diffusely, and (3) heat transfer by conduction in the tangential direction is negligible. Restriction (1) is commonly realized in this shelled spacecraft. Restriction (2) is approximated by many surfaces. Restriction (3) is not realistic for metal structures, but it may be observed that conduction in typical thin-skinned spacecraft can permit gradients of the order of 100°C or larger.

The solar absorptance and emittance of the outer surface are a and e_1; the emittance of the inner surface is e_2. In Figure 9, a sphere is shown which defines the geometry of the thermal balance. Because of symmetry, the temperature will be a function of angle θ, and isotherms will be defined by those circular strips for which θ is a constant as shown in the figure. The area of a circular strip is $2\pi r^2 \sin\theta\, d\theta$. The solar radiation absorbed by it is given by $2\pi r^2 \sin\theta \cos\theta\, sa\, d\theta$. The inner surface of this element will receive and absorb radiation from the remainder of the sphere. Because of the spherical shape and the diffusely emitting inner surface, the radiation per unit area incident on all inner surface elements is identical. This incident radiation per unit area on the inner surface is black body radiation corresponding to the mean of fourth power of the temperature of the sphere, σT^4; and the radiant energy absorbed by the inner surface of a circular strip is given by $2\pi r^2 \sigma e_2 T^4 \sin\theta\, d\theta$. The radiation emitted by both sides of the circular strip is $2\pi r^2 \sigma (e_1 + e_2)\, T^4 \sin\theta\, d\theta$. The statement of thermal balance for the circular strip, after cancelling the factor $2\pi r^2 \sin\theta\, d\theta$ common to all terms, is

$$Sa \cos \theta + \sigma e_2 \overline{T}^4 = (e_1 + e_2)\, T^4 \qquad (12)$$

$\overline{T}^4$, the root mean fourth power of the a sphere, can be obtained from equation (8) setting $k = 0$,

$$\overline{T}^4 = \frac{sa}{4\sigma e_1} \qquad (13)$$

and substituting (13) in (12) gives

$$sa \cos \theta + \frac{sae_2}{4e_1} = \sigma (e_1 + e_2)\, T^4$$

$$T^4 = \left(\cos \theta + \frac{e_2}{4e_1}\right) \frac{sa}{\sigma (e_1 + e_2)} \qquad (14)$$

The maximum temperature occurs for $\theta = 0$, corresponding to the spacecraft subsolar point. The hemisphere defined by $\theta = \pi/2$ to $\theta = \pi$ is an isothermal one at the minimum temperature; this result follows from the fact that no external radiation is received by this region and the internal radiation is uniformly incident. The magnitude of the variation for this spherical shell can be expressed as the ratio of

T^4 $(\theta = 0)$ to T^4 $(\theta = \pi/2)$,

$$\frac{T^4(0)}{T^4_{(\pi/2)}} = \frac{1 + \frac{e_2}{4e_1}}{\frac{e_2}{4e_1}} = \frac{4e_1}{e_2} + 1 \qquad (15)$$

as follows from equation (14).

The ratio for a few interesting cases is hown in the next table.

a	1.	1.	.2	.2	.1
e_1	1.	1.	.2	.2	.025
e_2	1.	0.2	0.2	1.0	0.5
$4e_1/e_2+1$	5.	21	5.	1.8	1.2
$T^4(0)$	151×10^8	213×10^8	151×10^8	89×10^8	277×10^8
$T^2(\pi/2)$	30×10^8	10×10^8	30×10^8	48×10^8	231×10^8
$T(0)^\circ C$	78	108	78	36	134
$T(\pi/2)^\circ C$	-38°	-95	-38	-7	117

The table indicates that low absolute values of the external surface a and e combined with a high absolute value for the emittance of internal surface yield the smallest gradients. The column at the extreme right corresponds roughly to the conditions applicable to the Echo I satellite. For this case, the assumption of negligible tangential conduction is realistic, and a gradient of the order of 30°C was anticipated. Without internal radiation exchange, the gradient could have exceeded 300°C.

The fourth factor to be considered for its effect on the radiation properties required for thermal balance is the period of time spent in the shadow of the earth and its relation to the heat capacitance of the spacecraft or spacecraft subsystem. Satellites are in orbit or will be placed in orbit in the next two years with shadow times ranging from approximately 30 minutes to six hours. While in the shade, the spacecraft loses energy at a rate depending on the thermal emittance of the external surface. Components in the interior will lose energy at a rate which depends, in addition, on the thermal impedance between the component and the surface. The use of vacuum insulation composed of a number of layers of aluminized mylar is one technique employed to increase the time constant. From the standpoint of radiation properties, it is evident that low absolute values of thermal emittance are suggested by long periods in earth shadow.

During the launch phase, the spacecraft is protected by the fairing of the vehicle. The fairing is heated aerodynamically and, in turn, heats the spacecraft by radiation. After removal of the fairing, the spacecraft is exposed to direct aerodynamic heating at a rate which depends on the altitude and velocity of the spacecraft. In the first of these two launch phases, the effect of heating from the fairing suggests a low absolute thermal emittance for the surface of the satellite. The second phase of direct aerodynamic heating suggests a high emittance in order to accelerate the re-radiation of absorbed energy.

There are several factors which may be designated as general design considerations which will have a direct bearing on the selection of solar absorptance and thermal emittance properties. Two general design factors are considered here: (1) the employment of active temperature control; (2) the use of a design which largely insulates the interior of the satellite from the external radiation and attempts to adjust the rate at which the internal heat is removed in order to achieve acceptable temperatures in the interior of the spacecraft.

An active temperature control system is one which adjusts one or more of three parameters: the solar absorptance, the thermal emittance, the thermal impedance between the temperature-controlled region and the exterior of the spacecraft. Adjustment of the solar absorptance or thermal emittance may be accomplished by a variety of mechanical schemes. In general, these make it possible to present one of two surfaces to the external incident radiation as absorbers of solar radiation or emitters of long-wave thermal radiation. Active temperature control systems generate a need for coatings with high and low absolute solar absorptances and for high and low thermal emittances.

The use of a thermal design which attempts to insulate the interior from the external radiation requires both high and low thermal emittance surfaces. No preference for low or high absorptance is made by this design.

The last group of factors to be considered relates (1) to the accuracy with which the radiation properties can be determined, (2) to the degree with which they can be reproduced, and (3) to the extent to which they change before, during, and after launch. The measurements of solar absorptance are least accurate for low

absolute values. When an optical method is used, the quantity measured is the reflectance as a function of wave length. For opaque materials, the reflectance is equal to (1 - absorptance). If care is exercised, reflectance can be measured to about one percent for normal incidence and specular surfaces. For highly reflecting surfaces such as evaporated gold and evaporated aluminum, an error of one percent in reflectance corresponds to an error of 5 to 10 percent in absorptance. The uncertainties in the measurement of thermal emittance generate a similar preference for coatings with high absolute values of emittance.

The problems of coatings' reproducibility and freedom from contamination due to pre-launch handling, as well as launch fairing outgassing, also suggest a preference for coatings with high absolute values.

Spacecraft Thermal Balance

When the external radiation sources are specified and internal dissipation defined, we can initiate the gross thermal balance needed for determining the average temperature. This part of the lecture will conclude with a brief statement of this process. In practice, extensive and detailed analyses requiring the use of large digital computers are employed to solve the numerous heat transfer equations which describe a spacecraft in sufficient detail, as will be shown by Mr. Kidwell in the second half of this lecture.

The relation for the isothermal heat balance is obtained by combining the radiation absorbed at the outer boundary and the internally generated heat as follows:

$$P_s\, a + P_a\, a + P_e\, e + P_i = A_{\sigma e} T^4 \qquad (15a)$$

where the new symbols are:

P_s = solar radiation incident

P_a = earth-reflected solar radiation

P_e = earth-emitted radiation

P_i = internal heat generated

The introduction of the earth-emitted radiation and internal power dissipation terms modifies the dependence of mean temperature on the a/e ratio. The dependence of mean temperature on a/e is shown in Figure 5 for spherical satellites with negligible internal dissipation. The significance of P_a plus P_e compared to P_s depends on the size and inclination of the orbit. P_a plus P_e will be negligible at altitudes of 20,000 miles. P_a is negligible when the normal to the orbital plane is coincident with the earth-sun line. For low orbits, e.g., 200 miles, and when 60% of the orbit is sunlit, P_a plus P_e can approach 40 percent of P_s. At 1000 miles, P_a plus P_e has dropped to 19 percent or less.

PART II

Spacecraft Thermal Design

The purpose of this part of the lecture is to describe in some detail how a thermal design is executed and to discuss some of the problems. The function of a thermal design is to maintain spacecraft temperatures within safe limits. Temperature tolerances are not always known accurately, but typical values are 0°C to 40°C for batteries and -10°C to +50°C for most electronic circuits. The median, 20°C, is normal room temperature.

There are two general methods, one passive and the other active, which are used to control spacecraft temperatures. With passive control, temperature is determined primarily by the properties of the external surfaces and the orbital environment. As the environment changes the temperatures also change. Active control systems regulate temperature by adjusting either the surface properties or the internal power dissipation.

There are two principal factors which can cause changes in the mean orbital temperature of a satellite. They are % time in sunlight, and attitude. For orbits close to the earth, the % time in sunlight can vary from 60% to 100% with the rotation of the orbital plane about the earth and the rotation of the earth about the sun. Average albedo inputs are maximum for the minimum sunlight orbit and vice versa, whereas the inputs from earth radiation are independent of the orientation of the orbital plane. The % sunlight factor, including earth radiation and albedo, can cause approximately 20°C variation in the mean temperature of a passively controlled satellite in a near earth orbit.

The solar energy absorbed by a satellite is proportional to its projected area normal to the sun. If the spacecraft structure is non-spherical, the absorbed sunlight is a function of solar aspect or attitude. Since the absorbed energy is the product of the solar constant, solar absorptance and projected area, attitude effects on temperature can be partially compensated by proper application of coatings with different absorptances. This

compensation cannot be complete. As an illustration, a cube with a uniform coating will absorb about 40% more energy at a 45° aspect than at an aspect normal to any face. Therefore, with compensation so that the maximum change in absorptance projected area product is 40%, the mean temperature of a passively controlled non-spherical satellite can vary as much as 30°C with attitude in an orbit far away from the earth.

Other factors which can contribute to uncertainties or fluctuations in mean temperature are tolerances in the a/e of the thermal coatings, variations in the solar constant and changes in internal power dissipation. A ±10% tolerance for the coatings and a ±3.5% seasonal variation in the solar constant cause 15°C and 5°C, respectively, total changes in mean temperature. Similar general estimates for internal power dissipation cannot be made because the temperature change depends on the total surface area and surface emittance. However, an example can be given. The temperature of a 3-foot diameter sphere with an emittance of 20% will vary about 0.5°C per watt.

The mean temperature factors can be summarized briefly.

% Sunlight (30%)	20°C
Attitude (40%)	30°C
Coatings (20%)	15°C
Solar Constant (7%)	5°C
Internal Power	- indefinite

If all effects are assumed to be cumulative under worst conditions, the following generalizations may be made regarding temperature limits of internal components, when internal power dissipation is neglected. A spherical satellite can be designed to operate within a 20°C temperature range away from the earth and a 40°C range near the earth. Similarly, a non-spherical satellite can be designed to operate in a 50°C range away from the earth and in a 70°C range near the earth. These, of course, are only generalizations and refer particularly to passively controlled satellites under worst conditions. On the other hand, mean temperature is only one consideration in a thermal design.

At this point, I would like to discuss the thermal designs of two satellites, the S-6 Atmospheric Structures Satellite, and the joint British-American Satellite, Ariel I.

S-6 Atmospheric Structures Satellite

Figure (10) shows the physical configuration which is a 3 ft. diameter stainless steel shell crammed full of mostly electronics, batteries, and supporting structure. The orbit parameters are 250 km perigee, 900 km apogee, and 64.3% to 100% sunlight. Internal power dissipation depends on command signals from tracking stations and can vary from zero to a maximum of 100 watts for 250 seconds, 12 times a day. This is equivalent to from 0 to 3.5 watts average power. The spacecraft is spin stabilized and is to have an expected lifetime of 120 days. 78.4% of the spherical surface is coated with an opaque coating of evaporated aluminum plus an overlay of 10 quarter wave lengths at 0.55 microns of evaporated silicon monoxide ($a = .17 \pm .01$, $e = .235 \pm .01$). The remaining 21.6% area is polished stainless steel ($a = .40 \pm .02$, $e = .12 \pm .01$). The average a/e is 1.04. Hemispheric values of absorptance and emittance are used.

Figure (11) shows mean temperature as a function of a/e for maximum and minimum sunlight orbits. Tolerances on a/e are estimated to be $\pm$ 6.5% by a root mean square calculation of individual tolerances rather than the worst combination of minimum and maximum values. When this tolerance is combined with the $\pm$ 3.5% seasonal variation in solar constant, the combined tolerance is $\pm$10%. Internal power of 3.5 watts will increase mean temperature about 1.5°C, so that flight temperatures are predicted to remain within limits of approximately 0°C to 30°C.

The stainless steel areas are distributed in eight circles centered about surface mounted electron temperature probes, pressure gages and mass spectrometers. This slightly non uniform distribution of the coatings should not cause more than 3°C change in mean temperature with solar aspect.

The choice of thermal coatings was restricted by the experimenters' requirements for a clean and conducting outer surface. Their preference was for a polished, stainless steel sphere sealed so that internally generated contaminants could not reach the instrument ports. The aluminum silicon-monoxide coating was acceptable except for its electrical insulating properties. The uncoated areas near the instruments satisfied the minimum requirements for a conducting surface. The coatings were applied by Dr. Hass of USAERDL, Fort Belvoir, Virginia, who first developed this technique for the Vanguard satellites.

Although mean temperature of the S-6 is almost independent of attitude, skin temperatures are not. Skin temperature gradients were minimized by blackening interior sphere surfaces and internal components to maximize radiation transfer. Computed gradients are 25°C between the equator and the poles when the sun shines broadside and 90°C between the poles when the sun shines down the spin axis.

Ariel I

Figure (12) is a photograph of Ariel I. It has an almost spherical epoxy-fiberglass structure, and it is powered by solar cells mounted on four paddles. The orbit parameters are perigee 370 km, apogee 1027 km, % sunlight 63% to 100%, and solar aspect, $\pm 45^{\circ}$ from the satellite equator. The major problems were: (1) temperature control of three experiments, the mass spectrometer which is the small sphere located forward of the main structure, the cosmic ray experiment which is located inside the dome beneath the mass spectrometer, and the electron temperature electronics, which is inside a large boom mounted cylinder, (2) the calculation of absorbed sunlight as a function of attitude because of the shading of one part by another, and (3) the thermal coatings.

The coatings were limited by the experimenters' requirement for a highly conducting surface to gold or rhodium with a minimal area painted for temperature control. The final coatings were 75% evaporated gold and 25% black and white paint. A

second requirement was for an antenna ground plane of several mils of copper between the fiberglass structure and the thermal coatings. Figure (13) shows how these coatings were built up. Starting from the fiberglass, the layers are (1) a sealing varnish, (2) a metallizing lacquer, (3) conducting silver paint, (4) electroplated copper, (5) and (6) the varnish and lacquer again, (7) evaporated gold, and (8) the paint. There is more art than science in coating techniques, but this process was developed to solve problems of adhesion, substrate boiling through outer layers when heated, and of providing a mirror like finish for the gold.

The shading problem was solved by taking photographs of a scale model of the satellite at approximately 80 attitudes about two axes. To satisfy the temperature limits of the experimenters, temperatures were computed at 30 points in the satellite as a function of solar aspect. The governing equations were programmed for an IBM 7090 computer and solved for a variety of coating patterns selected on a trial and error basis

Figure (14) shows a plot of % time in sunlight, solar aspect, and mean temperature of Ariel I as a function of days after launch. It should be noted how closely the temperature follows the % time in sunlight and also that the temperatures run from about room temperature to nearly 50°C. These temperatures are running about 4°C higher than the maximum values computed on the basis of +10% tolerance for the coating properties and solar constant combined and about 12°C higher than computations based on measured values. As a matter of interest this is one of the satellites which was exposed to radiation from the high altitude atomic test last July.

The Thermal Model

The heart of a thermal design is the thermal model, an approximate mathematical representation of the spacecraft. It consists of a set of from one to 50 or more equations describing the heat transfer among the selected points or nodes of a structure. The selection of nodes is governed partly by convenience in working around interfaces, partly by accuracy requirements, and partly by a desire to minimize engineering and computer time. Figure (15) shows a cutaway drawing of

Explorer XII and Figure (16) shows the location of nodes in the thermal model.

The heat flow at each node may be described by the following equation.

$$(mc)_i \frac{dT_i}{dt} = a_i P_{si} + a_i P_{ai} + e_i P_{ei} + P_i - A_i \sigma e_i T_i^4 - \sum_{j=1}^{N} K_{ij} (T_i - T_j) - \sum_{j=1}^{N} A_i \sigma F_{ij} (T_i^4 - T_j^4) \quad (16)$$

where i, j = $i^{\underline{th}}$ and $j^{\underline{th}}$ nodes
$(mc)_i$ = thermal capacity
T_i = temperature, absolute
t = time
a = solar absorptance
P_s = incident solar power
P_a = incident albedo
P_e = incident earth radiation
P_i = internal power dissipation
A = surface area
σ = Stefan-Boltzmann constant
e = emittance
K = thermal conductance
F = radiation exchange factor
N = number of nodes or equations

It is noted that this equation allows for heat stored, inputs from sunlight, albedo, earth radiation and internal power, radiation to space, and both conduction and radiation among nodes. Most of these coefficients are written symbolically. The major effort in a thermal analysis is to supply the numerical values for these coefficients.

Equation (16) represents a system of N equations in N unknowns to the first and fourth powers for which there is no analytic solution. Under equilibrium conditions and when conduction may be neglected each dT/dt and K equals zero and the transformation

(17) $$Z = T^4$$

results in a system of algebraic equations in Z which can be solved by matrix algebra. However, in general, conduction is appreciable and non-equilibrium solutions are required so that approximate methods must be used. If the fourth power terms are approximated by the first two terms of a Taylor expansion

(18) $$T^4 \cong T_o^4 + 4T_o^3(T - T_o)$$
$$= 4T_o^3 T - 3T_o^4$$

If

(19) $$Y = T_o$$

then

(20) $$T_i^4 \cong 4Y_i^3 T - 3Y_i^4$$

Then under equilibrium conditions equation (16) reduces also to a system of algebraic equations of the form

(21) $$[C_{ij}] \times [T_i] = [D_i]$$

where

$$C_{ij} = -K_{ij} - 4A_i\sigma F_{ij} Y_j^3, \qquad (i \neq j) \tag{22}$$

$$C_{ii} = \sum_{j=1}^{N} K_{ij} + 4A_i\sigma e_i Y_i^3 + \sum_{j=1}^{N} 4A_i\sigma F_{ij} Y_i^3, \qquad (i=j) \tag{23}$$

$$D_i = \alpha_i (P_{Si} + P_{ai}) + e_i P_{ei} + P_i + 3A_i\sigma e_i Y_i^4 + \sum_{j=1}^{N} 3A_i\sigma F_{ij} (Y_i^4 - Y_j^4) \tag{24}$$

The solution of equation (21) is only accurate as the approximation of equation (20). The solution can be obtained to any accuracy simply by the following iterative process. Initially arbitrary values of say 300°K are assumed for each Y_i, then trial values of T_i are obtained from the first solution. Then for the second solution, the T_i's from the first solution are used for the Y_i's. Three iterations are required to reduce the error within 0.1°C if the initial estimates are not off more than about 50°C.

Transient solutions can be obtained in a similar manner with matrix algebra simply by approximating the derivatives by

$$\frac{dT}{dt} \cong \frac{T(t+\Delta t) - T(t)}{\Delta t} \tag{25}$$

It is not necessary to use the iterative technique to gain accuracy, and equation (25) becomes simply

$$\frac{dT_i}{dt} \cong \frac{T_i - Y_i}{\Delta t} \tag{26}$$

where Y_i is the solution for T_i for the previous time interval. The matrix method has an advantage over the usual finite difference methods in that it is always stable.

These equations are easily programmed for a digital computer. Once a program is available all that should be necessary for thermal design studies is to feed in the non-zero coefficients of equation (16) and wait for the answers.

Temperature Gradients - Explorer XIV

Figure (17) shows a picture of Explorer XII which was physically almost identical to Explorer XIV. The orbit is highly eccentric and the satellite is in sunlight almost all of the time. The problem areas in the thermal design were (1) the transmitter which is mounted on a plate at the base of the spacecraft, (2) the magnetometer which was located at the end of the forward boom, (3) large changes in power dissipation, (4) the possibility of up to 5 hours in shadow, and (5) large solar aspect changes coupled with a highly non-spherical structure. The only restrictions on the thermal coatings was that electrical conduction paths which circle the magnetometer be broken.

Figure (18) shows the temperatures at four locations, the magnetometer, transmitter, battery and encoder for the first 150 days in orbit. The battery and encoder are located on an equipment shelf which is the region inside the octagon shaped area. The solar aspect varied from 25° to 165° referred to the forward direction of the spin axis. It should be noted that the transmitter and magnetometer temperatures vary much more than the battery and encoder. Figure (19) shows temperature transients during a two hour shadow period. Thus far, including both solar aspect and shadow effects, the transmitter has experienced temperatures from $+60^{\circ}C$ to $-35^{\circ}C$.

Launch Phase

Transient heating or cooling and contamination of temperature control surfaces and surface-mounted equipment are the two major problems during launch. There is radiation from nose cone inner walls during ascent through the denser air and then after nose cone ejection, there is direct aerodynamic heating on the spacecraft's forward surfaces. Then there can be a transition period where the vehicle may coast

for minutes or hours until the last stage is fired (or restarted) to inject the satellite into orbit. Figure 20 shows calculated temperatures of the solar paddles on Explorer XII while tied down against the sides of the third stage.

The outgassing from a heated nose cone may condense on payload surfaces and substantially alter the properties of optical surfaces and sensors. Figure 21 shows the Explorer X magnetometer inside the Delta nose fairing. It also shows the thermal coatings of evaporated aluminum and aluminum paint which were designed with an a/e of 1.6 to operate the magnetometer sphere at 40°C in a highly eccentric orbit. The magnetometer malfunctioned in orbit when its temperature reached equilibrium at 60°C. Later, from simulated tests with heated nose cone samples, it was demonstrated that contamination approximately doubled the absorptance of the evaporated aluminum and thereby caused the failure. For Explorers XII, XIV and XV, either Teflon* or an ablator was applied to the outer fairing surfaces to reduce contamination levels. For Ariel I, both an ablator on the outside and a Teflon shield on the inside were used.

Design Verification

Many aspects of a thermal design require experimental tests for: (1) evaluating conduction across interfaces; (2) observing temperature gradients in complex equipment and spacecraft structures; and (3) checking thermally optical measurements of coating properties. In addition, there should be full systems tests of a complete satellite in a simulated space environment. To verify the thermal design, solar simulation is required. Unfortunately, the accuracy of current solar simulation facilities is not sufficient for this purpose. Telemetered data from orbiting spacecraft provide the only independent verification of a thermal design.

*Reg. Trade Mark

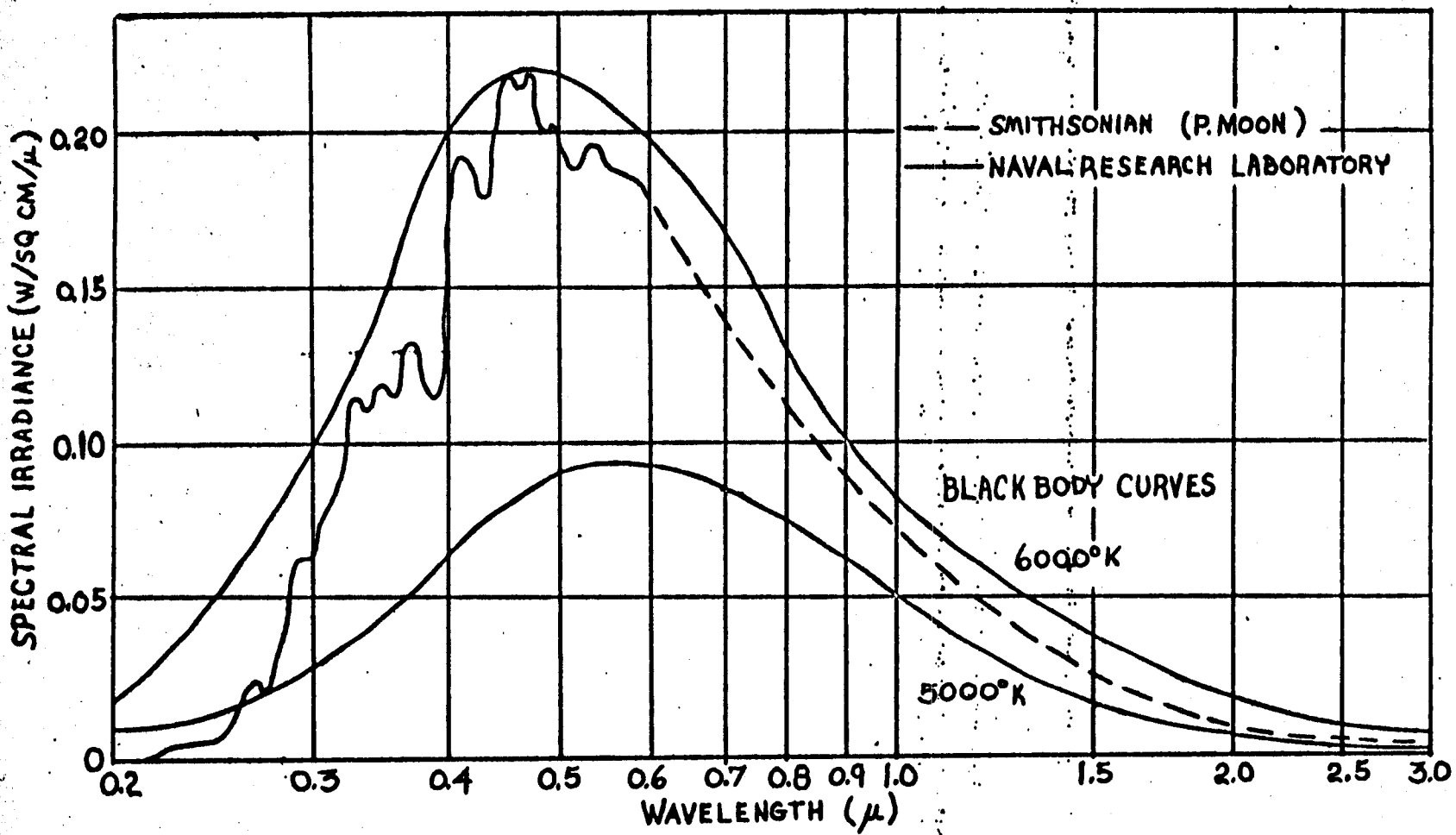

Fig. 1 - The Complete Solar Spectral Irradiance Curve from 0.22 μ to 3 μ and Black Body Radiation Curves for 5000°K and 6000°K.

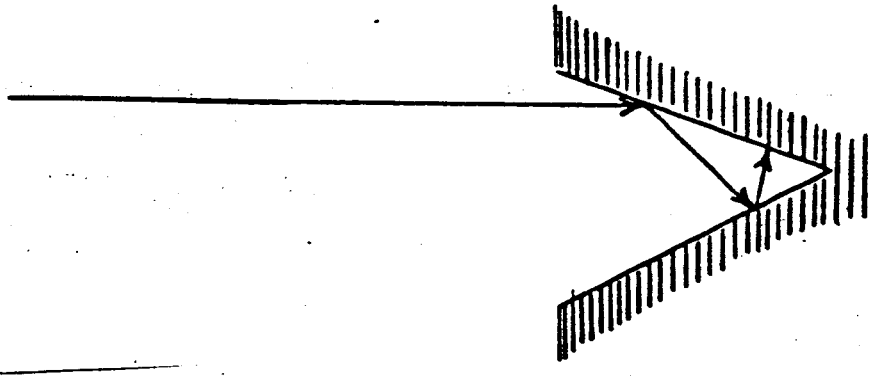

Multiple Reflection and Absorption by a Wedge

Figure 2

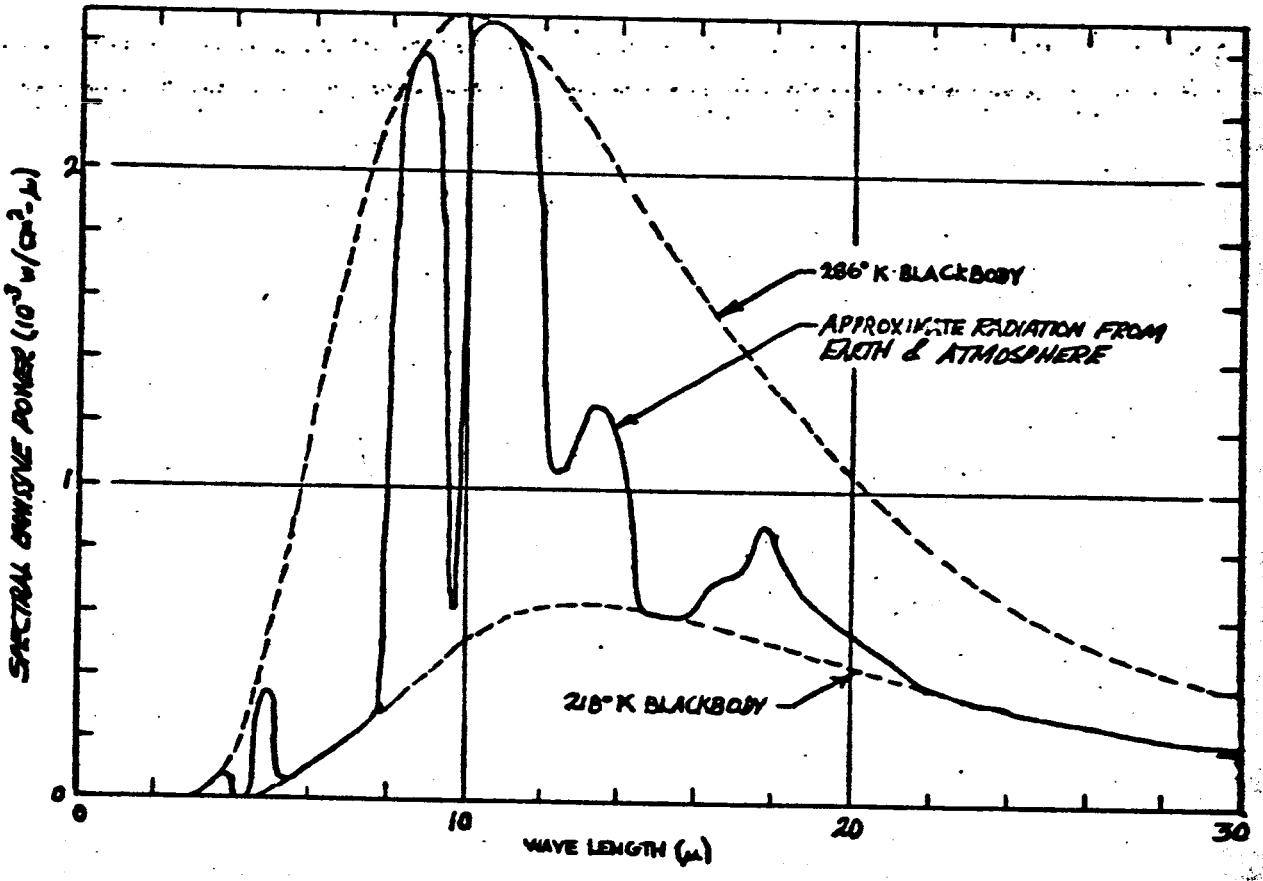

Blackbody Spectral Intensity Distribution and Estimate of Earth-emitted Radiation Returned to Space

Figure 3

PERCENT TIME IN SUNLIGHT

DEC. 21 (WINTER SOLSTICE) JUNE 21 (SUMMER SOLSTICE): ADD 12 HOURS 3 MINUTES.

FOR TWO WEEK FUTURE CONDITIONS: ADD 6^h0^m FOR THE 200-800 MILE ORBIT OR ADD 4^h50^m FOR THE 200-1500 MILE ORBIT.

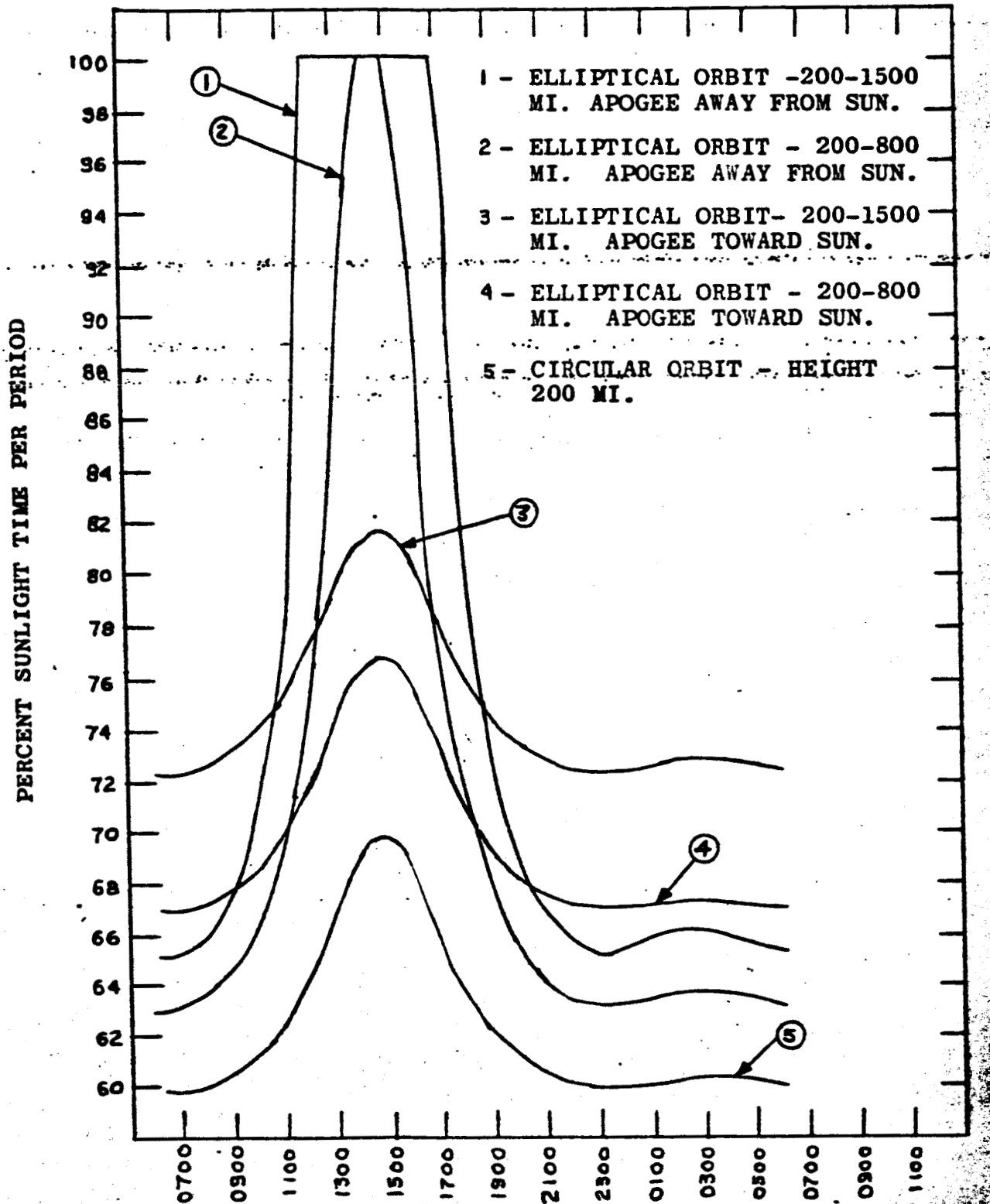

Figure 4

MEAN ORBITAL SHELL TEMPERATURE OF A SPHERICAL SATELLITE VERSUS RATIO OF TOTAL SOLAR ABSORBTIVITY TO THERMAL EMISSIVITY, α/ϵ

	A	B	C
ORBIT	200-1500 MILE	200-1500 MILE	200 MILE CIRCLE
% TIME IN SUN	100	75	60
LAUNCHING DATE	WINTER	WINTER	SUMMER
% CLOUD COVER	100	100	0
ALBEDO %	50	50	20

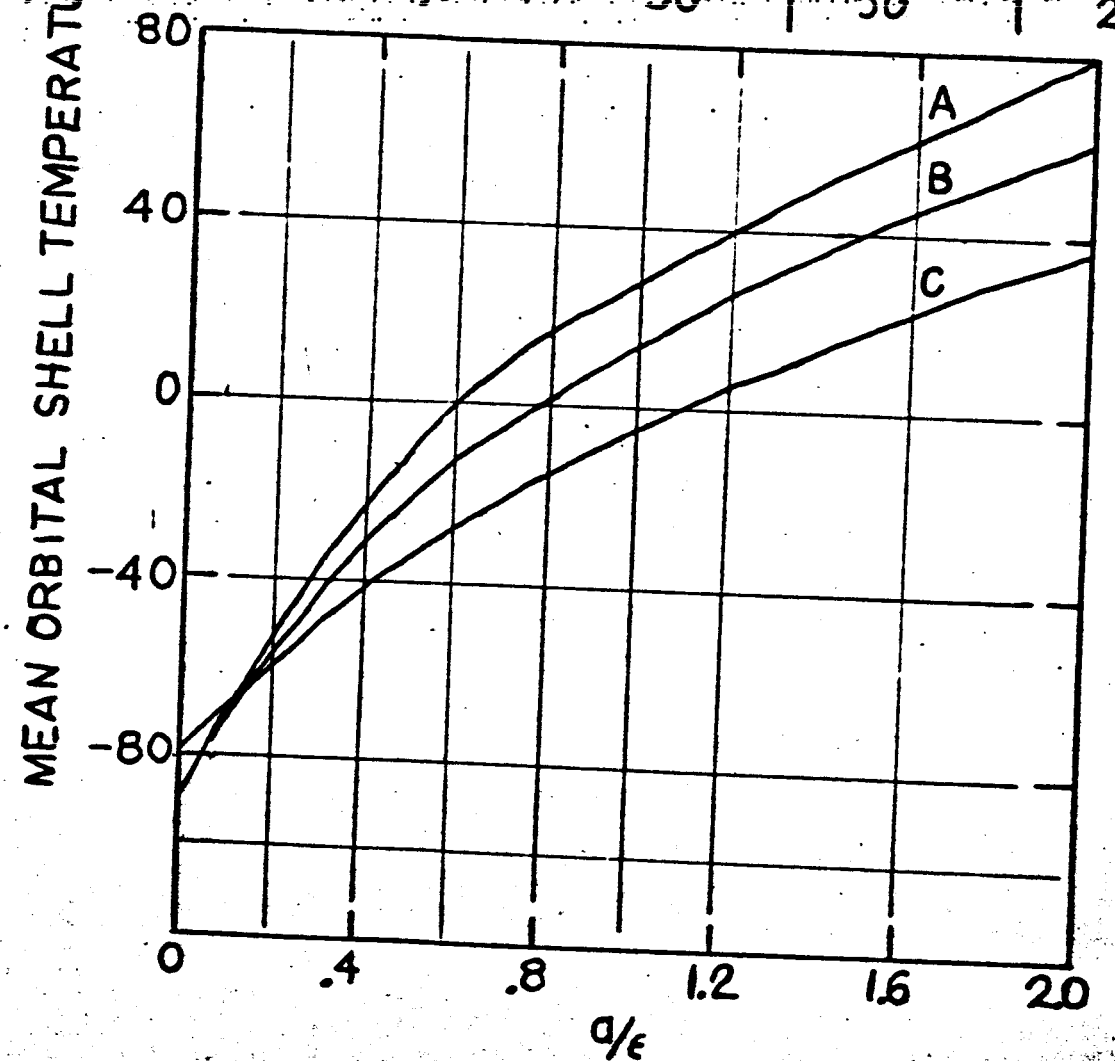

Figure 5

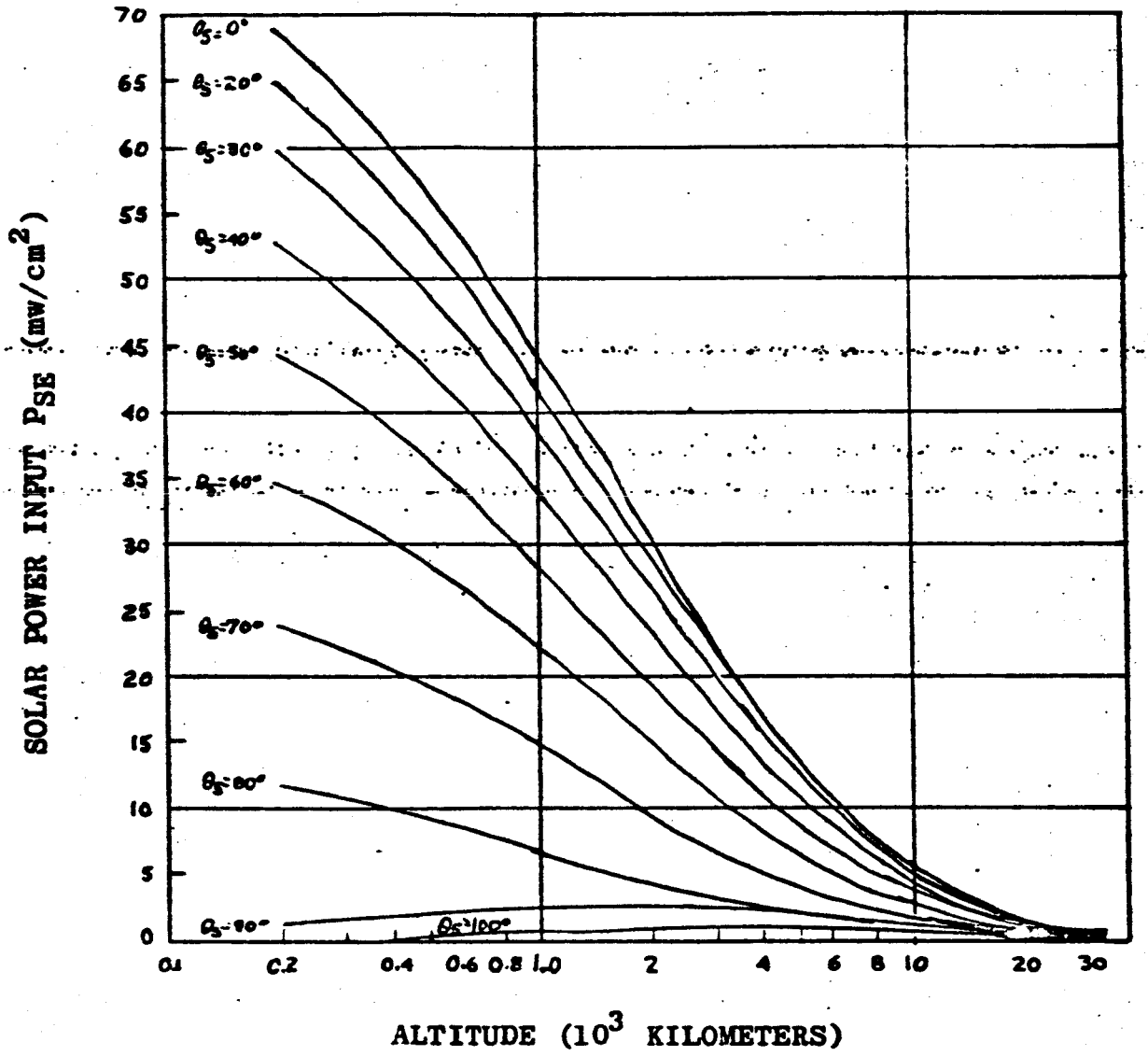

Figure 6 - Incident Earth-reflected Solar Radiation per Unit Cross-sectional Area of a Spherical Satellite Plotted as a Function of Altitude for the Range 200-32,000 km

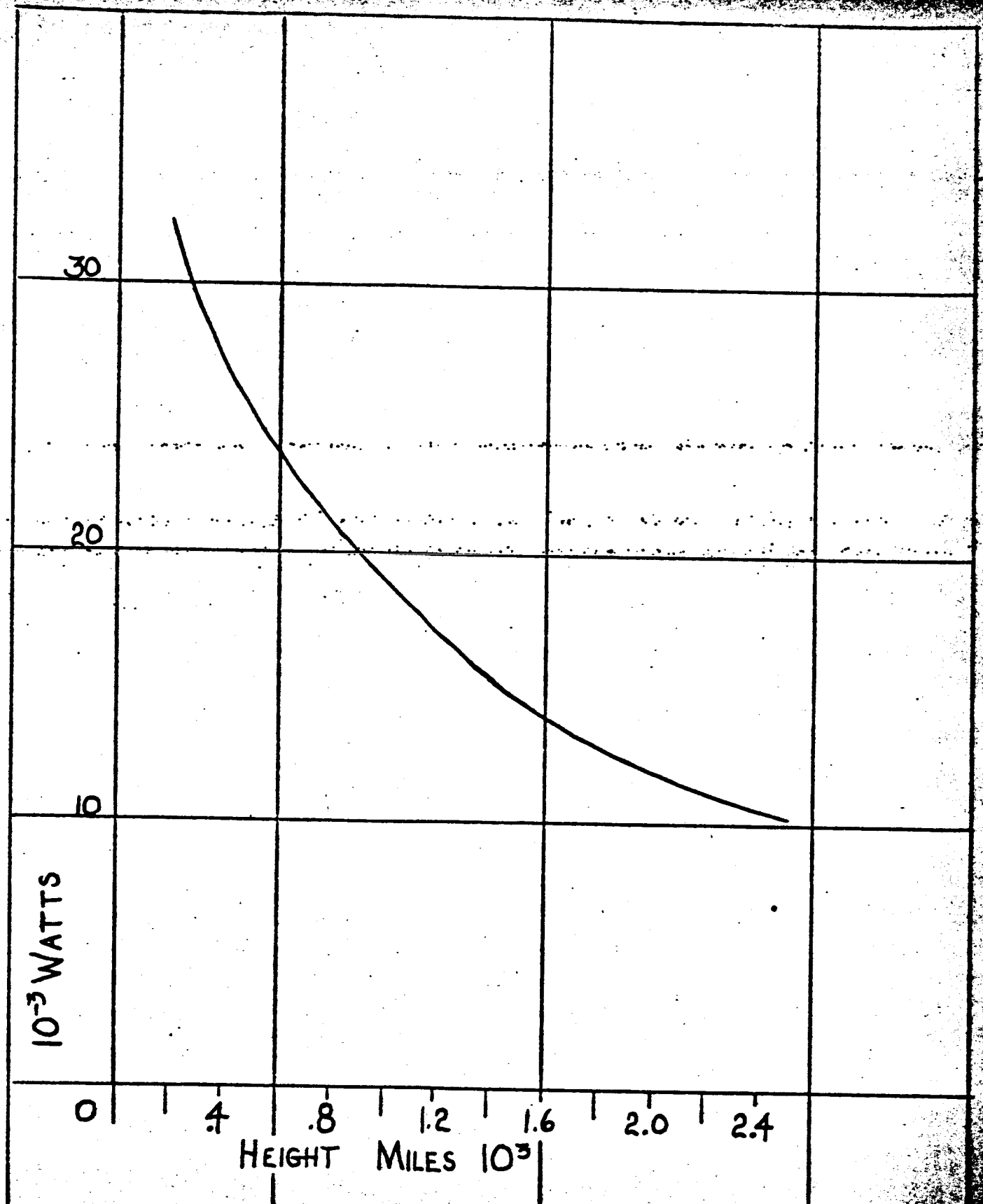

Figure 7

Incident Earth-Emitted Radiation per Unit Cross-Section Sphere

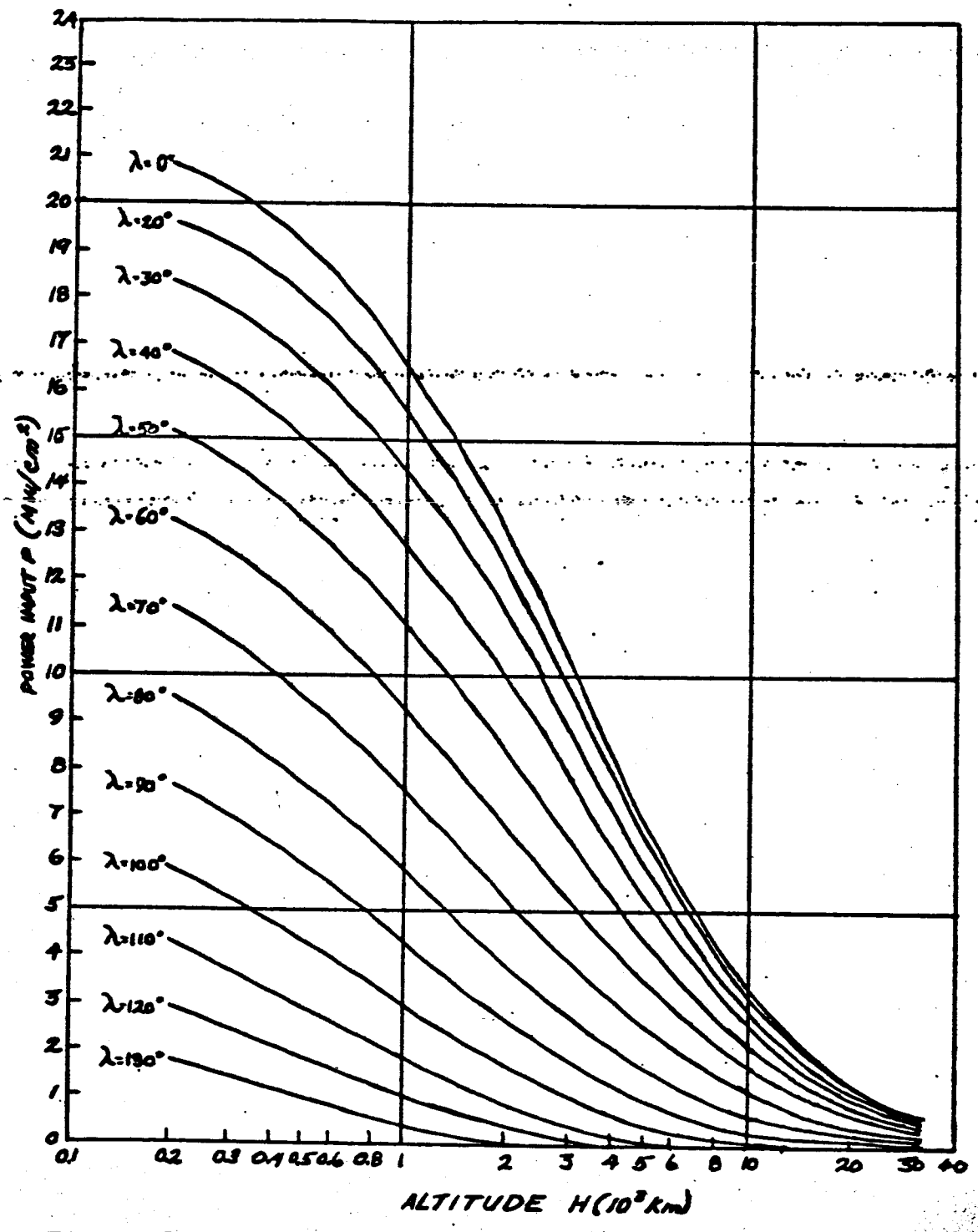

Figure 8 - Earth-emitted radiation incident on a flat plate as function of altitude for various angles between the normal to the plate and the line between earth center and the plate normal.

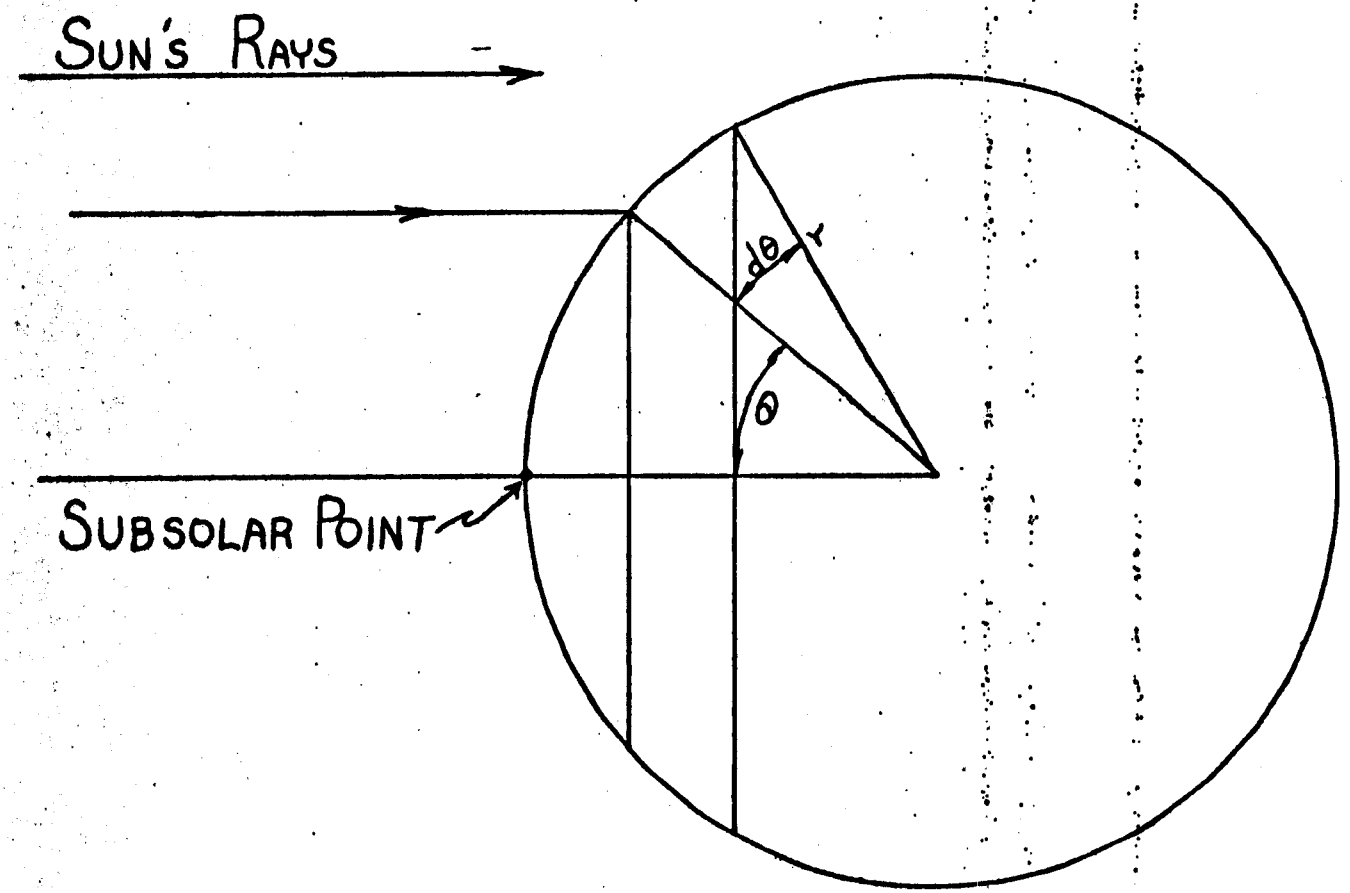

FIGURE 9 SOLAR RADIATION INCIDENT ON SPHERICAL SHELL

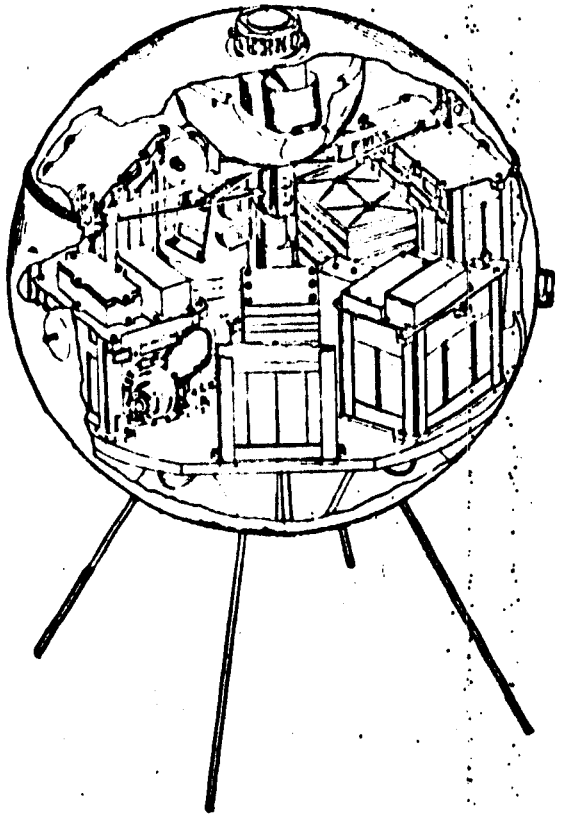

Figure 10 — S-6 atmospheric structure satellite, interior arrangement

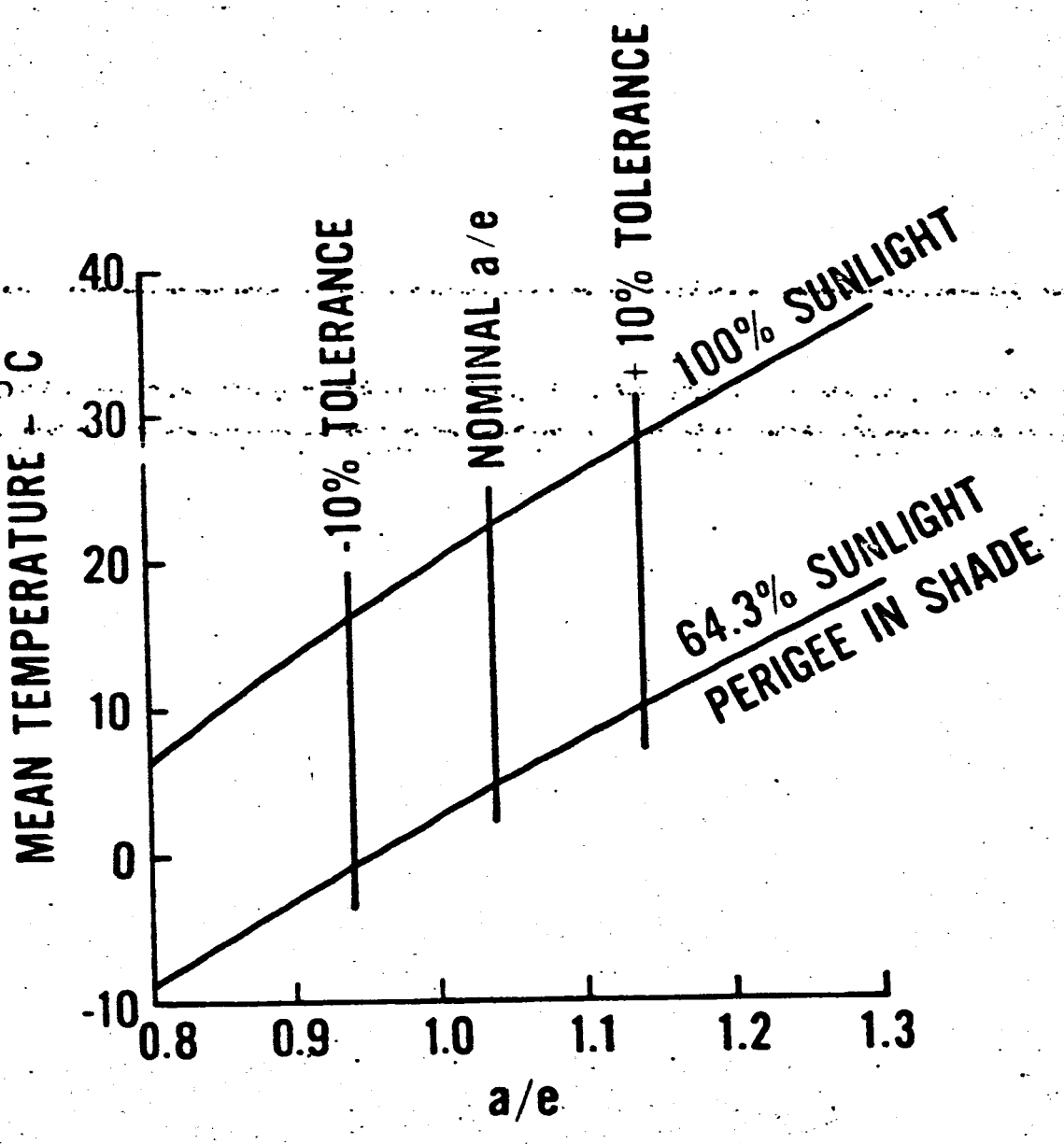

Figure 11 — S-6 mean temperature vs a/e

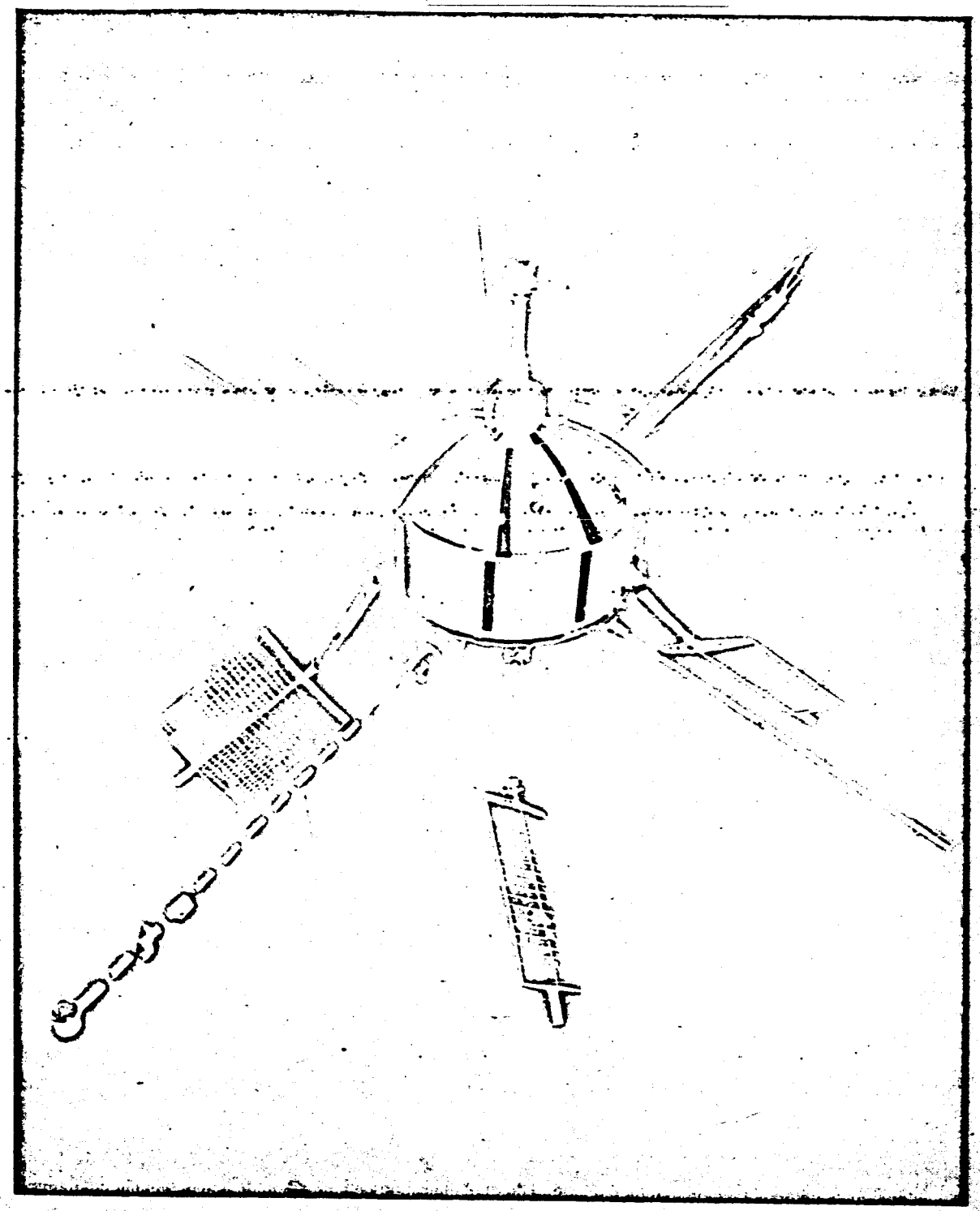

Figure 12 — Ariel I photograph

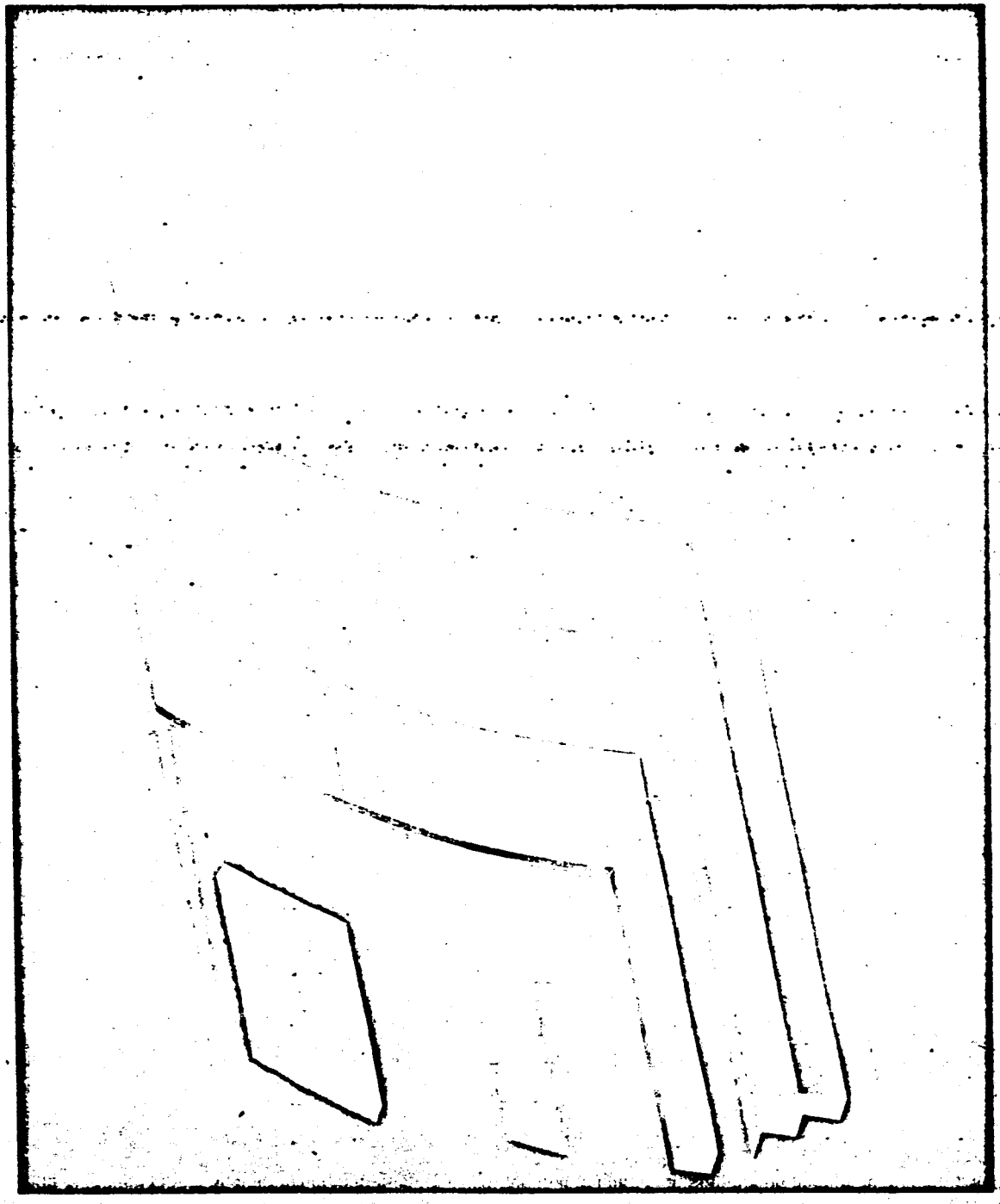

Figure 13 — Ariel I coatings

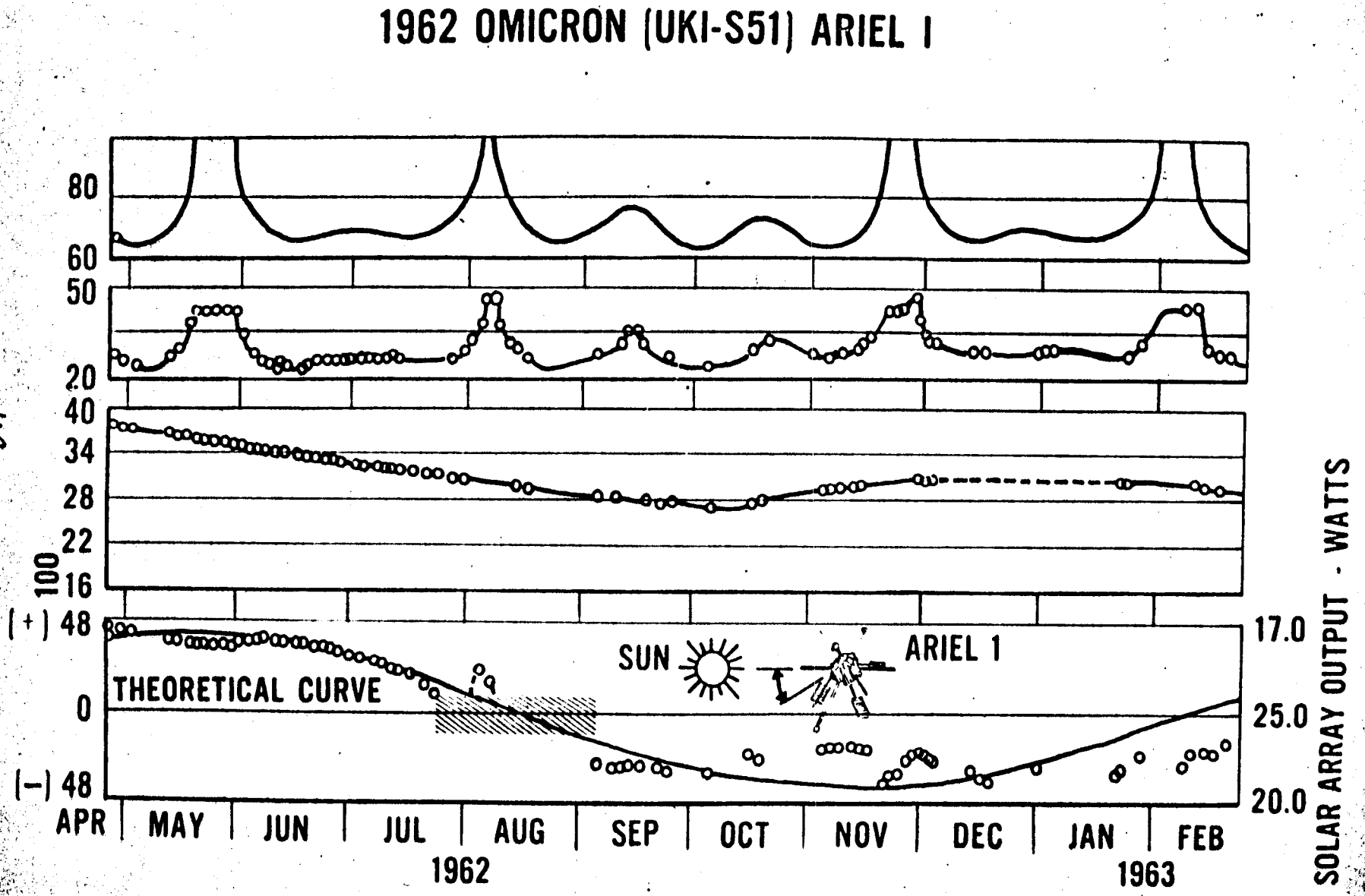

Figure 14 — Ariel I flight temperature

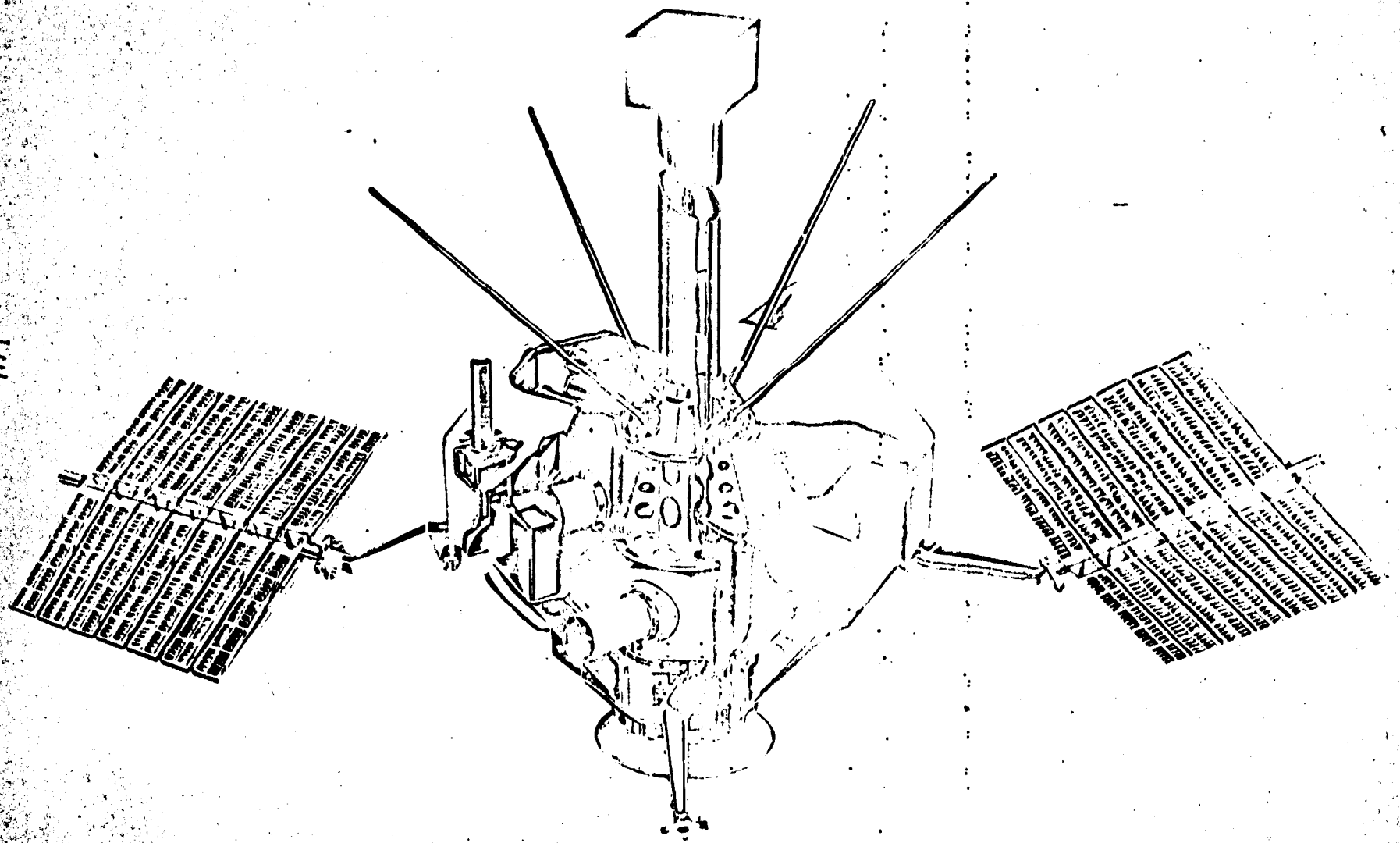

Figure 15 — Explorer XII cutaway

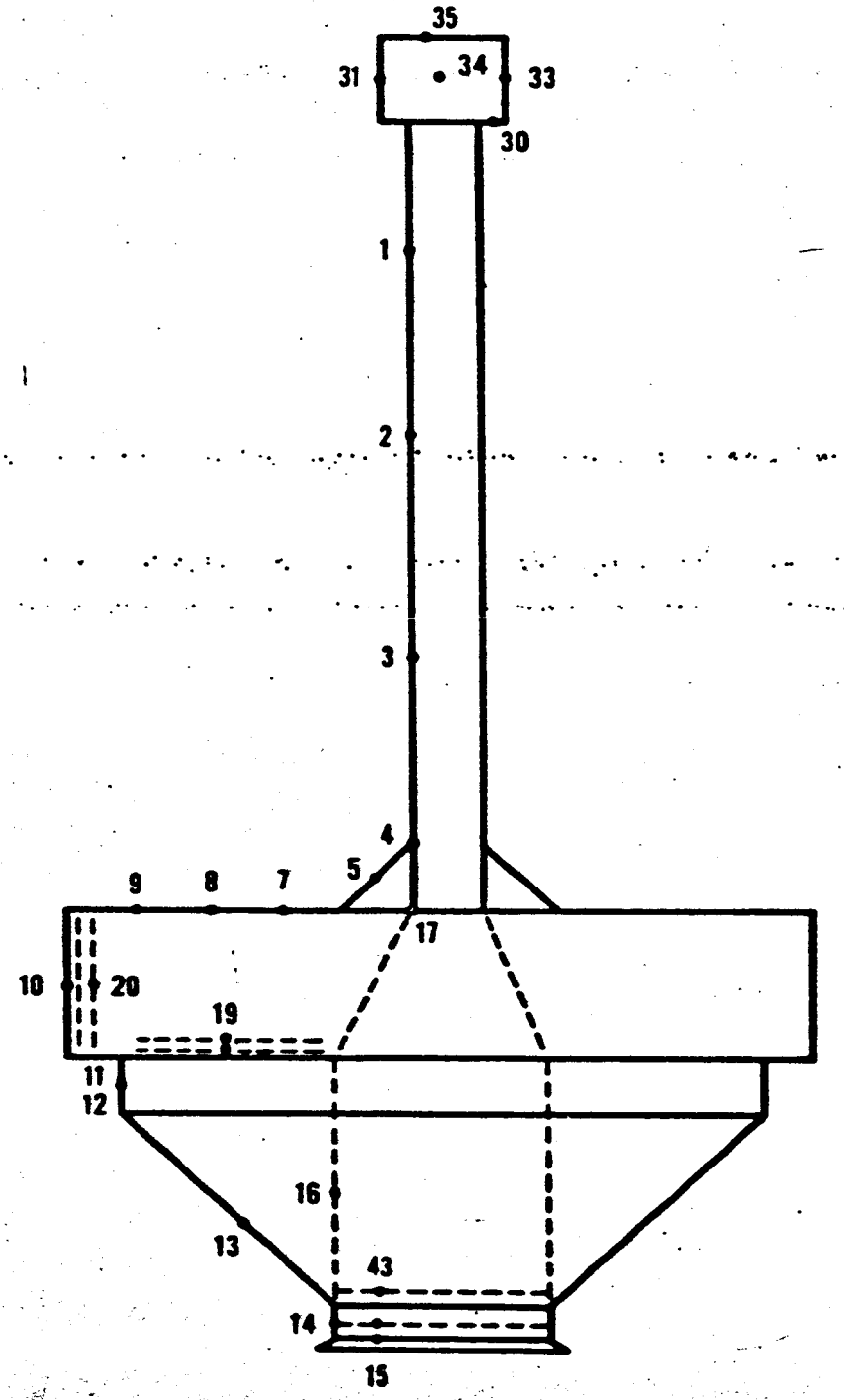

Figure 16 — Explorer XIV thermal model

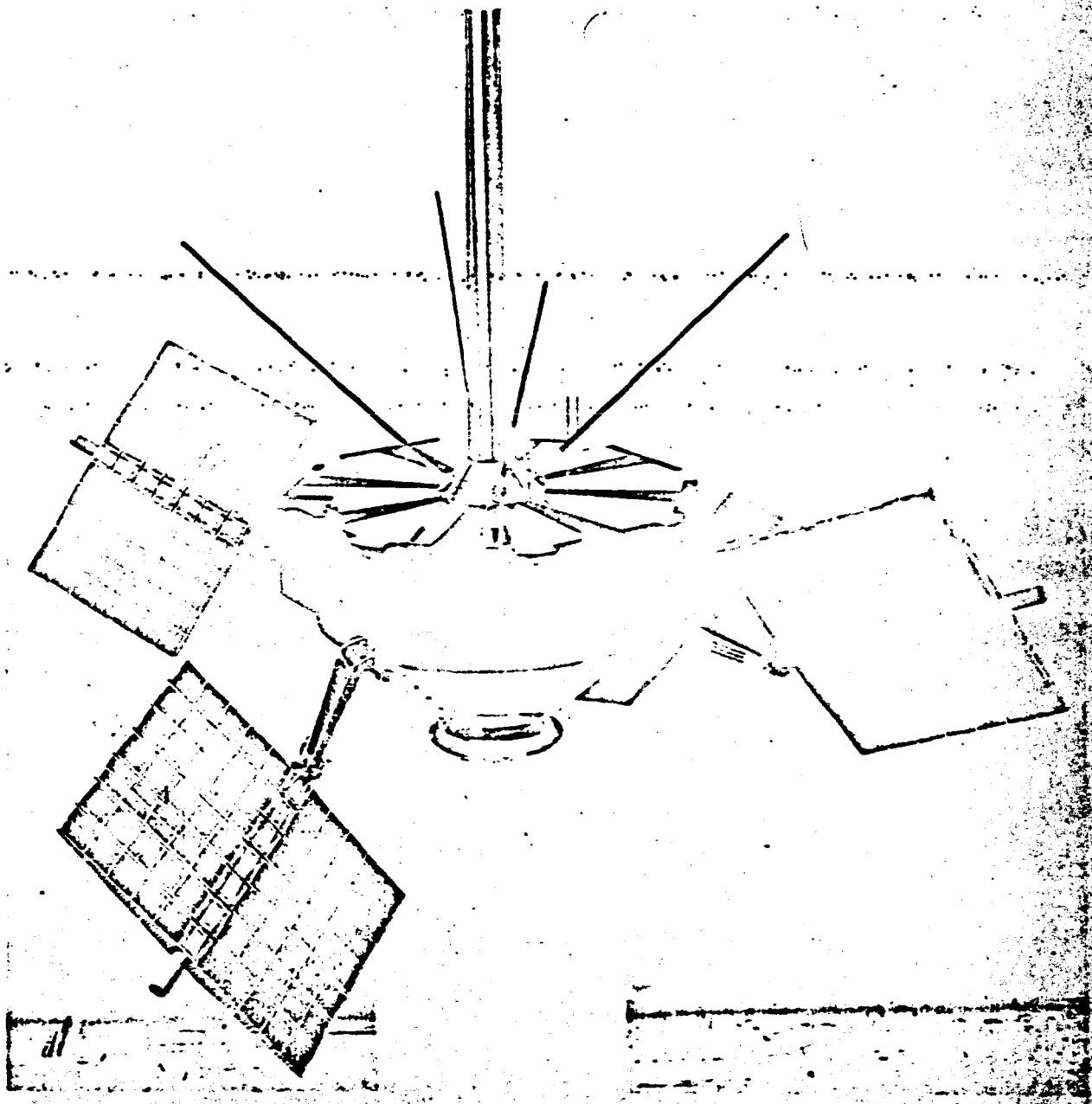

Figure 17 — Explorer XII thermal coatings

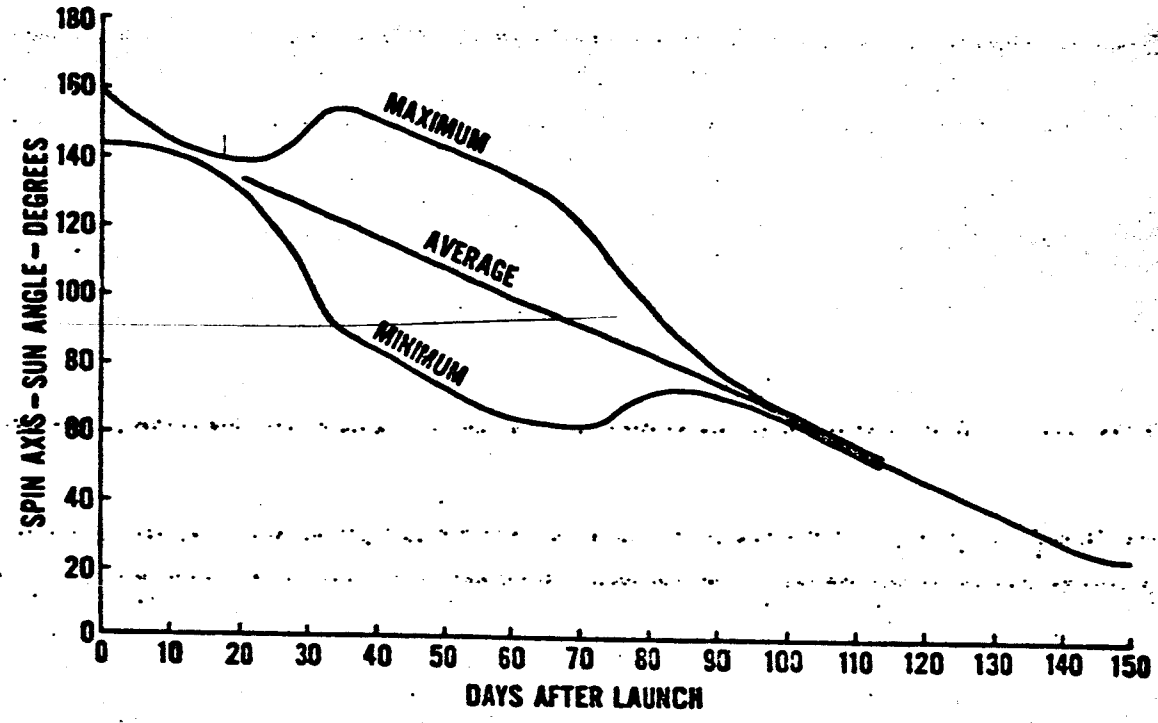

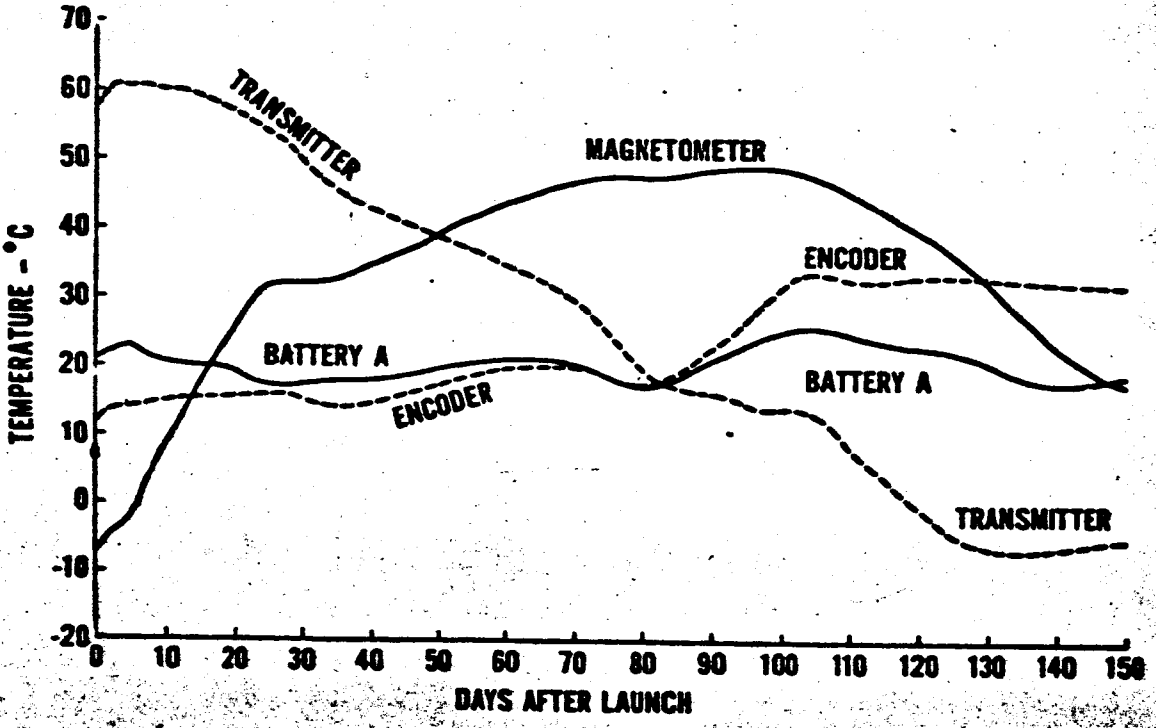

Figure 18 — Explorer XIV temperature data

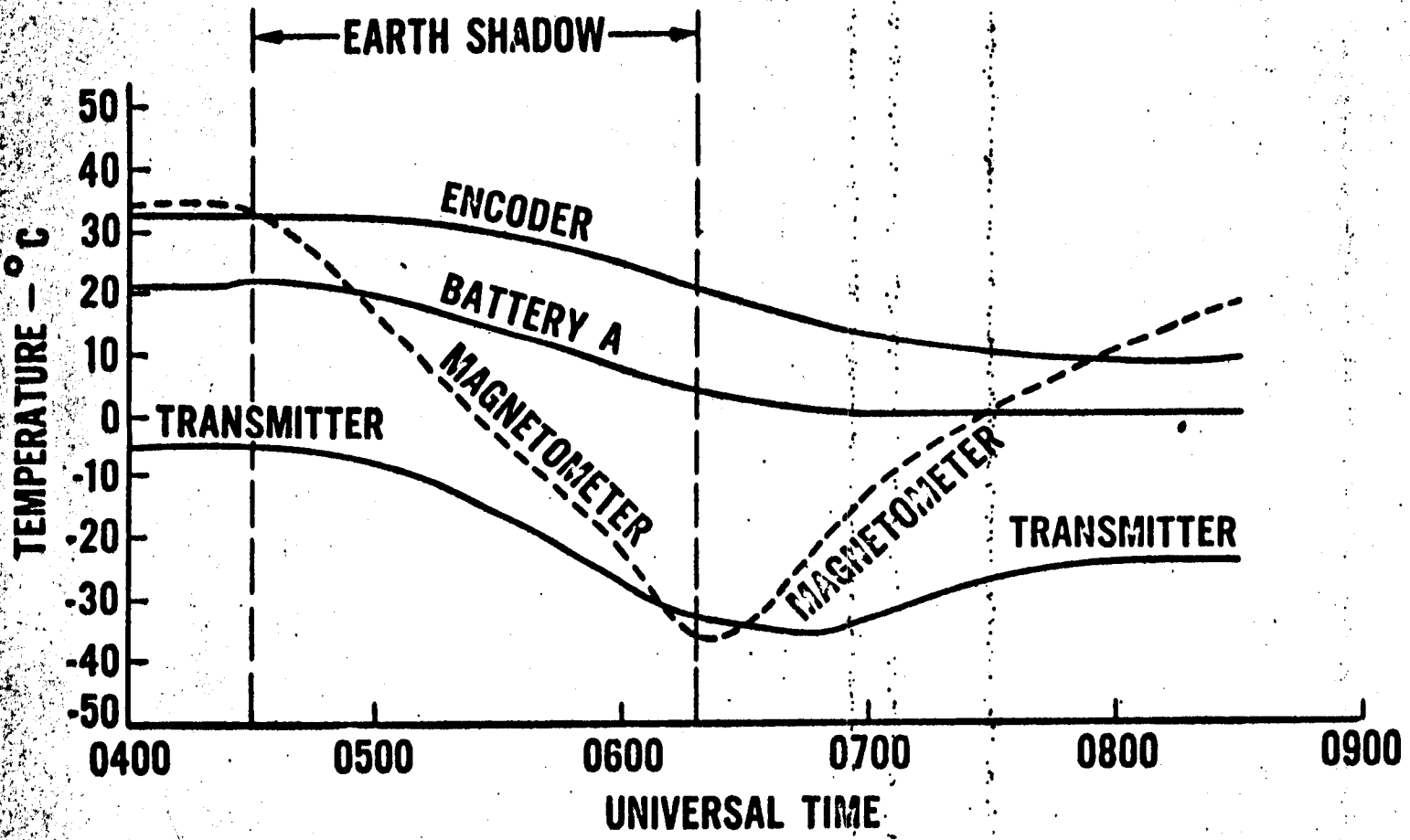

Figure 19 — Explorer XIV temperatures during shadow period

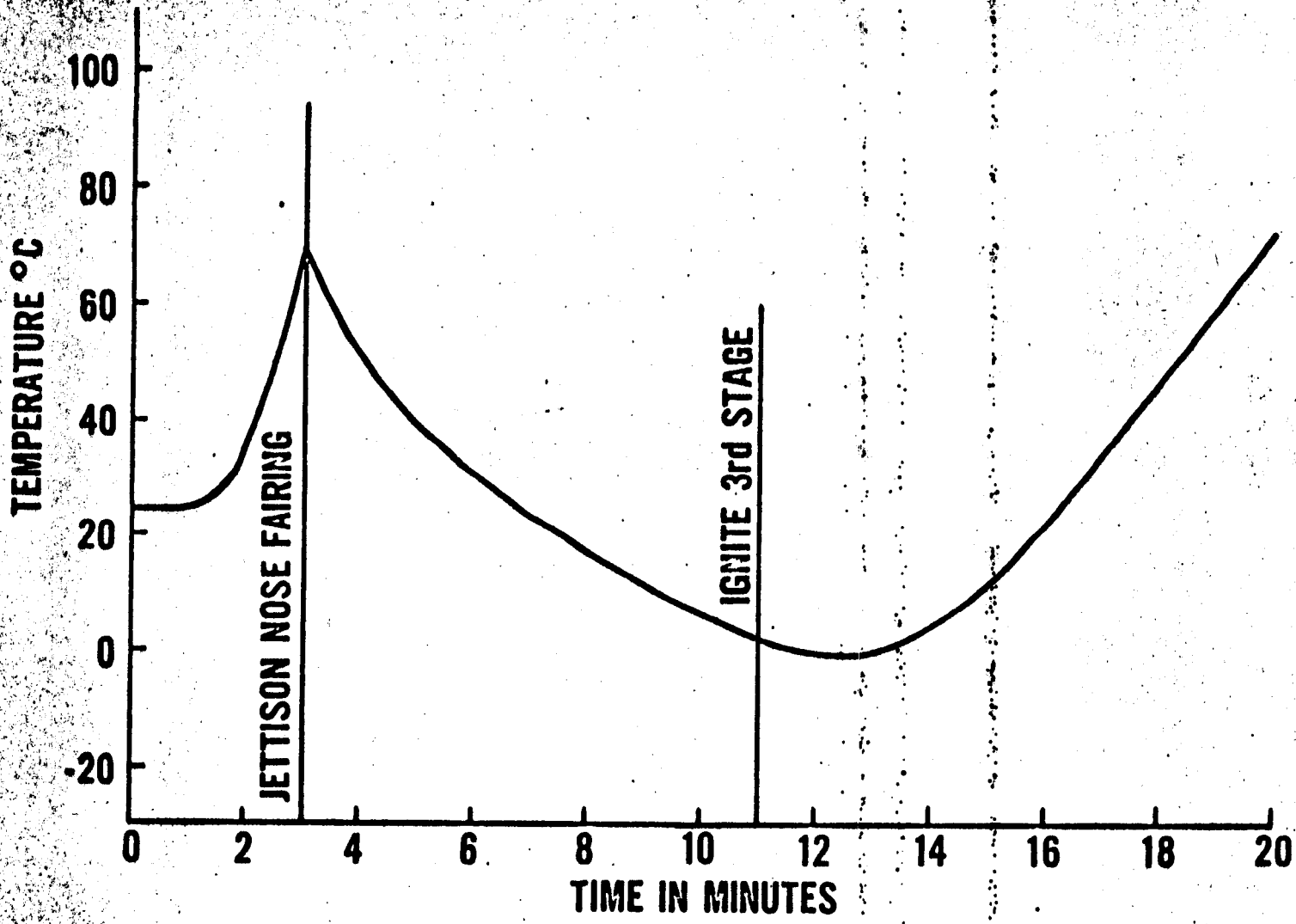

Figure 20 — Explorer XII solar paddle temperature during launch

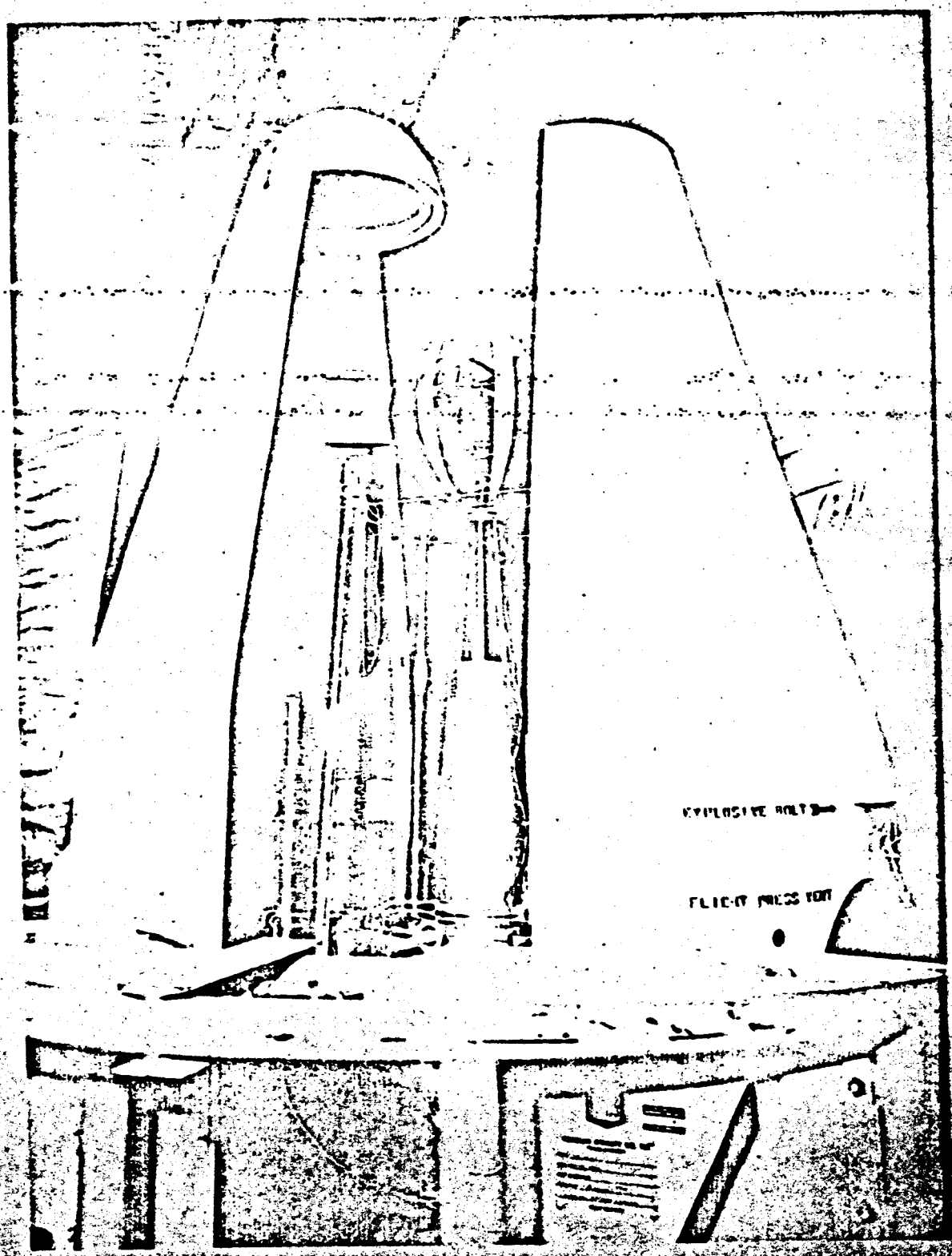

Figure 21 — Explorer X inside Delta fairing

REFERENCES

1. Francis S. Johnson, The Solar Constant, Journal of Meteorology, Vol. 11, No. 6, Dec. 1954, p. 431-439.

2. John C. Johnson, Physical Meteorology, John Wiley and Sons, N.Y., 1954, Chapters 2, 4 and 5.

3. Henry G. Houghton, The Annual Heat Balance of the Northern Hemisphere, Journal of Meterology, Vol. II, No. I, Feb. 1954, p. I-9.

4. J. Siry, R. Wilson, et al., NRL Report 5066, Mar. 1958.

5. G. Hass, L. Drummeter and M. Schach, Temperature Stabilization of Spherical Satellites, Journal of the Optical Society of America, Vol. 49, No. 9, Sept. 1959, p. 918-924.

6. F. Cunningham, Earth Reflected Solar Radiation Input to Spherical Satellites, ARS Journal, July 1962, p. 1033-1036.

7. F. Cunningham, NASA Tech. Note D-710, Power Input to a Flat Plate from a Diffusely Radiating Sphere, Aug. 1961.

8. F. Kreith, Radiation Heat Transfer, International Textbook Company, 1962.